REGULATION OF PROTEIN SYNTHESIS IN ADULT RAT CARDIOMYOCYTES

by

Brandon Pei Han Huang

H.B.Sc., The University of Toronto, 2005

A THESIS SUBMITTED IN PARTIAL FULFILLMENT OF
THE REQUIREMENTS FOR THE DEGREE OF

MASTER OF SCIENCE

in

The Faculty of Graduate Studies

(Biochemistry and Molecular Biology)

The University of British Columbia

(Vancouver)

May 2008

Abstract

Protein synthesis (mRNA) is tightly regulated under numerous conditions in cardiomyocytes. It can be activated by hormones such as insulin and also by other agents such as phenylephrine (PE) that activates hypertrophy in the heart. Cardiac hypertrophy involves an increase in the muscle mass of the heart, principally in the left ventricular muscle, and the increase is due to enlarged cell size, not increased cell number. A pivotal element of cardiac hypertrophy is an elevation in the rates of protein synthesis, which drives the increase in cell size causing hypertrophy. Unfortunately, we currently lack the understanding of the basic mechanisms that drives hyperactivated protein synthesis. Cardiac hypertrophy is clinically important because it is a major risk factor for heart failure. It initially serves as an adaptive response to increase cardiac output in response to higher demand, but ultimately leads to deterioration of contractility of the heart if hypertrophy is sustained. The main goal of this research project is to understand how hypertrophic agents, such as phenylephrine (PE), activate protein synthesis using adult rat ventricular cardiomyocyte as a model. Specifically, this study focuses on how the translational initiation is controlled by upstream signalling pathways.

Table of Contents

List of Tables

List of Figures

Acknowledgements

I would like to thank Dr. Chris Proud for providing me with lots of guidance and support during these exciting and memorable three years in his lab. Under his supervision, I have developed as a scientist and a person.

I have to say thank you to past and present members of the Proud laboratory for being my role models and providing a great working atmosphere in the lab. I especially would like to thank Dr. Yanni Wang (my golden partner) and Dr. Xuemin Wang (the corner stone of the Proud lab). Without them, I would not be able to achieve what I have done in another three years.

Finally, I would like to dedicate this M.Sc. thesis to my mother, Su-Chin Huang. Her lunch boxes kept me through the dark times and I am very grateful for her unconditional support.

Chapter 1

Introduction

1.1 Protein Synthesis/mRNA translation

Proteins are the cellular components involved in almost all biological processes in a cell. From the synthesis of cell membrane to DNA replication, all aspects of cellular activities are highly dependent on proteins to perform efficiently and correctly. Due to the high demand for proteins, much of the energy in a cell is committed to protein synthesis. In brief, protein synthesis is a process which involves translating a messenger RNA, which contains the genetic information copied from DNA, into a polypeptide. Producing a protein is not a trivial task. It requires several energy-demanding steps which involve an extensive set of biological machinery such as the ribosomes and translation factors. Ribosomes consist of multiple proteins and ribosomal RNAs (rRNA) and normally exist in the cytoplasm as two subunits, 40S and 60S, which are named according to their sedimentation rates through a density gradient.

mRNA translation is conventionally divided into three stages: initiation, elongation, and termination (see Figure 1.1). During translation initiation, the 40S ribosomal subunit is recruited to the 5' end of the mRNA where it is joined by the 60S ribosomal subunit to form the 80S ribosome with the help from multiple initiation factors. During translation elongation, ribosomes are the molecular machines by which amino acids are connected through peptide bonds. When the peptide chain is completed, the 80S ribosome dissociates from the mRNA into 40S and 60S subunits and is recycled for another round of translation. Since protein synthesis is such a sophisticated and costly process, it is under tight regulation at all three stages, especially in the initiation stage,

where specific mRNAs are selected for translation and before the cell commits any significant amount of energy into the process. The extensive regulation of mRNA translation allows the rapid modulation and fine-tuning of gene expression without transcription and the mRNA processing steps.

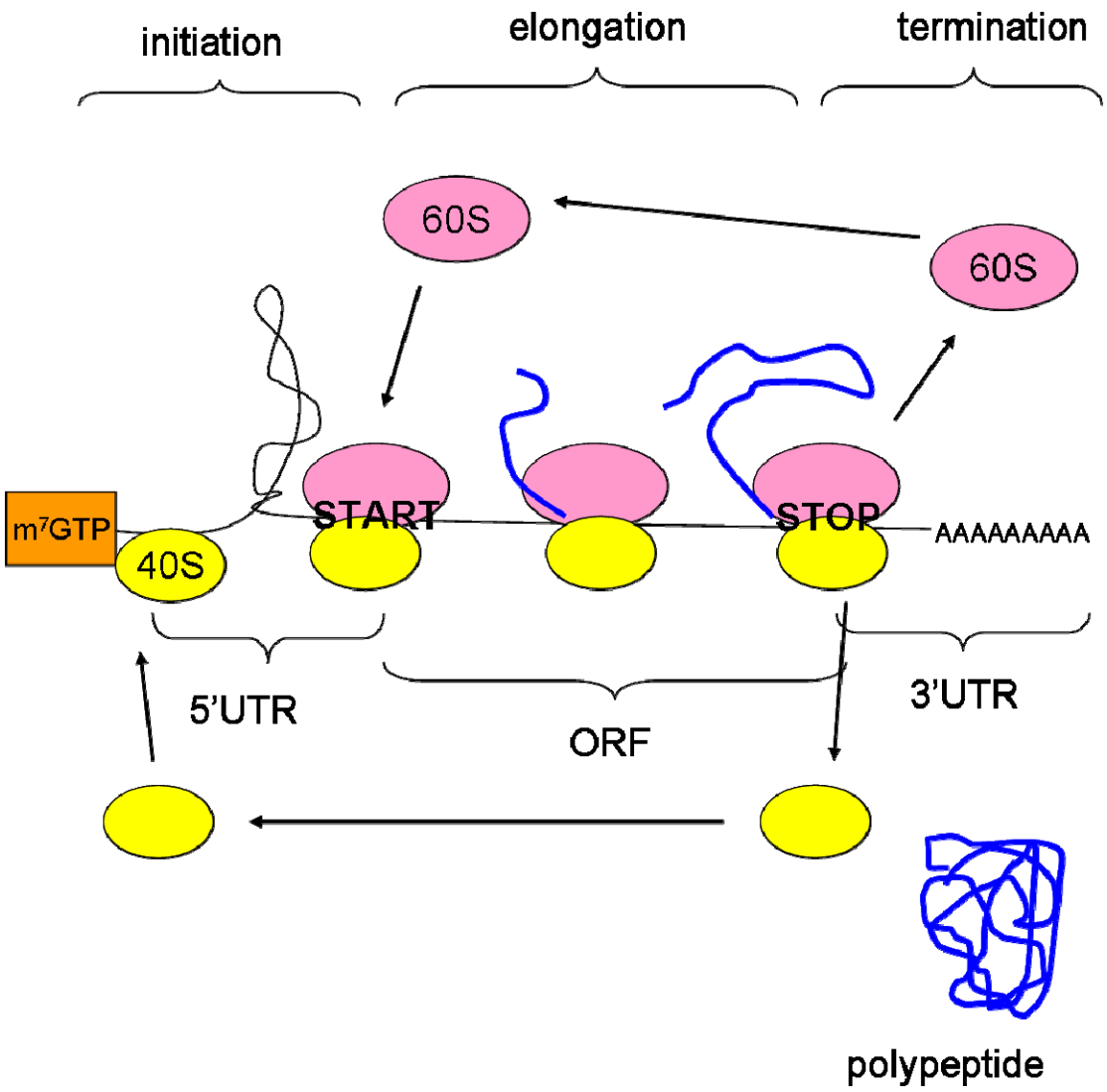

FIGURE 1.1. Schematic diagram of the three stages of mRNA translation. The 40S and 60S ribosomal subunits are indicated as "40S" and "60S", respectively. The mRNA contains a 5'-terminal m7GTP cap structure ("m^7GTP"), the initiation codon ("START"), the open reading frame ("ORF"), the 5'-untranslated region ("5'UTR"), the 3'-untranslated region ("3'UTR"), the termination codon ("STOP") and a polyadenylated tail ("AAAAA…"), as indicated. Translation initiation involves recruitment of the ribosomal subunits to the mRNA and delivery of the initiator methionyl-tRNA to the correct initiation codon (the later process is not shown in this diagram). Elongation involves the delivery of the correct aminoacyl-tRNAs to the ribosome, peptide bond formation and the translocation of the ribosome along the mRNA. Termination involves the recognition of the stop codon and the release of the newly formed polypeptide chain and the ribosomal subunits.

1.2 Translation Initiation: mRNA recruitment to the ribosome

One of the most crucial events during translation initiation is the binding of the to-be-translated mRNA to the ribosome. Binding of ribosomes to most cellular mRNAs strongly depends on the 5' m^7GTP cap structure (a 7-methylguanosine moiety) (Kozak, 1999) although there are exceptions (viral or stress protein mRNAs) that contain intrinsic ribosome-interacting elements in their 5' untranslated regions (5'UTRs). The importance of the 5' cap was demonstrated by Shatkin et al. (Shatkin and Banerjee et al., 1976) who showed that translation absolutely requires the methylated guanosine at the 5' terminus of mRNA. 5' m^7GTP cap of an mRNA functions to facilitate the assembly of initiation complexes including the small ribosomal 40S subunit at the 5' UTR. This step is mediated by the eukaryotic initiation factor 4F (eIF4F) complex, which contains eIF4E, eIF4G, and eIF4A (Gingras and Raught et al., 1999; Kozak, 1999). eIF4G is a large scaffold protein that holds all the components of eIF4F complex together and interacts with numerous other proteins to promote efficient initiation of translation. These proteins include poly(A) binding protein (PABP) which allows mRNA circularization, eIF3 for interaction with the 40S ribosomal subunit, and the Mnks, the kinases that act on eIF4E. eIF4E binds the 5' m^7GTP cap and thus provides a physical interaction between the eIF4F complex and the mRNA. Once eIF4F binds to an mRNA, the translational apparatus is brought onto the mRNA to begin translation. Therefore, the binding of eIF4F to the 5' m^7GTP cap of an mRNA is believed to be a critical regulatory step for both general and specific mRNA translation because it determines whether or not a particular mRNA is

translated.

Assembly of eIF4F complex is regulated by a family of small polypeptides, the eIF4E-binding proteins (4E-BPs) (see Figure 1.2). Among the members, 4E-BP1 is the best understood and actually is the only form expressed in adult ventricular cardiomyocytes (ARVC). The binding of 4E-BP1 to eIF4E precludes the interaction between eIF4E and eIF4G and 4E-BP1 thus acts as a competitive inhibitor of translation initiation (Gingras and Raught et al., 1999). 4E-BP1 and eIF4G binding to eIF4E is mutually exclusive because they share a common sequence motif that interacts with eIF4E (Mader and Lee et al., 1995). The affinity of 4E-BP1 towards eIF4E is regulated by its phosphorylation status such that 4E-BP1 dissociates from eIF4E upon phosphorylation (will be discussed later in this chapter). eIF4E is also subject to phosphorylation by the Mnks, however, its influence on eIF4E's affinity towards 5'm7GTP cap is unclear (Tuxworth and Saghir et al., 2004).

The 5'UTR of cellular mRNAs may contain secondary structures that limit the interaction between mRNA and the 40S ribosomal subunit. To overcome this obstacle, eIF4A, an ATP-dependent RNA helicase, unwinds the mRNA structures to provide an unstructured platform for the binding of ribosomes to facilitate unobstructed translation initiation (Rozen and Edery et al., 1990). eIF4A usually works in tandem with eIF4B and eIF4H which enhance eIF4A's RNA helicase activity. Both of these companions boost eIF4A's activity (Richter-Cook and Dever et al., 1998; Rogers and Richter et al., 1999). It is widely believed that eIF4F could be essential for the efficient translation of highly

structured mRNAs (Kimball, 2001).

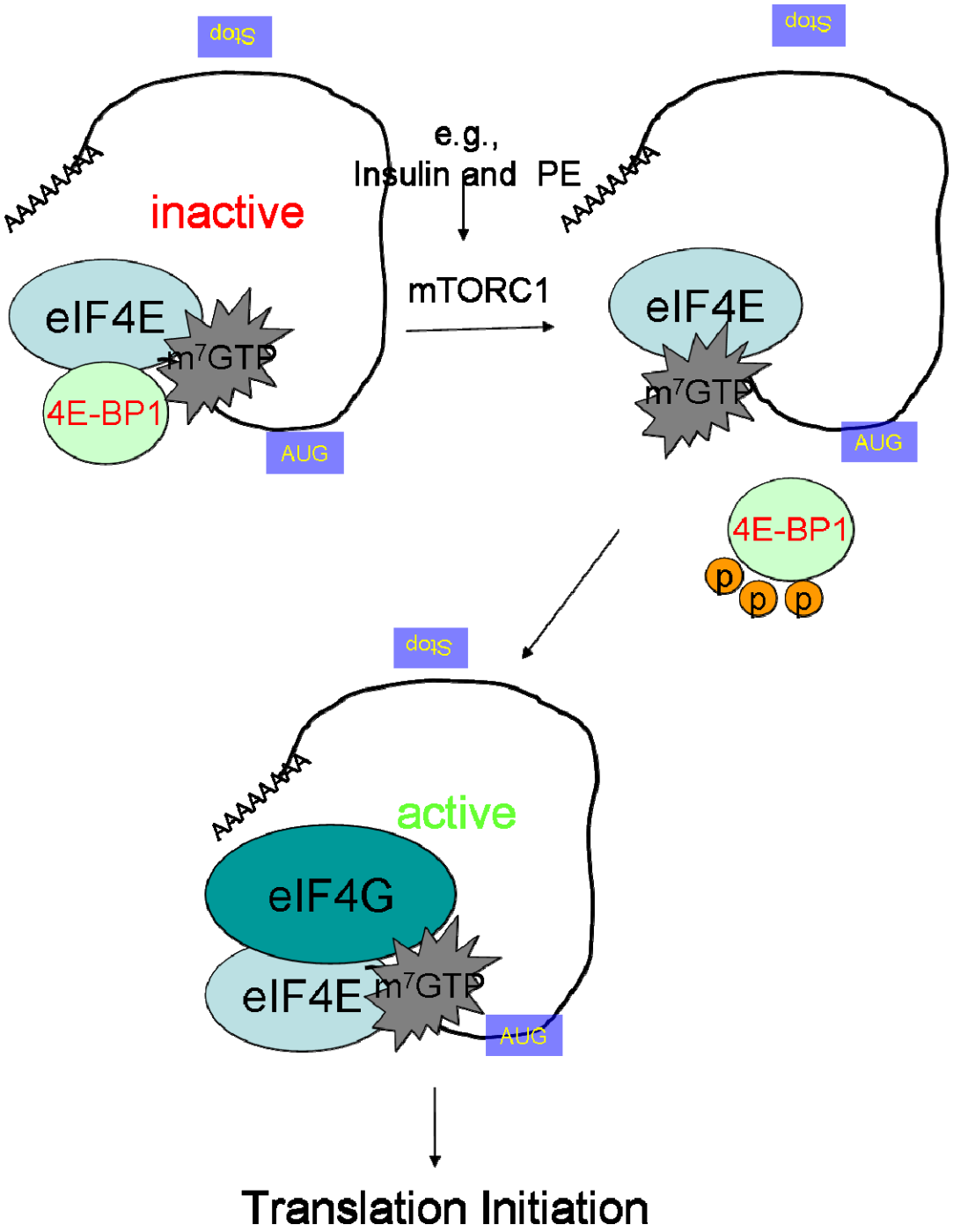

FIGURE 1.2. Diagram depicting a current model of translation initiation mediated by the eIF4F complex.

By binding to eIF4E, 4E-BP1 prevents the interaction between eIF4E and eIF4G causing the mRNA to remain translationally inactive. Upon mTORC1 stimulation by insulin or PE, 4E-BP1 becomes phosphorylated and dissociates from eIF4E. The exposed eIF4E becomes available for eIF4G, which then recruits the translational machinery (not shown) and turns on initiation of mRNA translation.

1.3 Regulation of 4E-BPs and eIF4F complex

As described earlier, the eIF4E-binding activity of 4E-BP1 is modulated by a series of phosphorylation at specific residues: Thr37, Thr46, Ser65, and Thr70 (Gingras and Gygi et al., 1999; Mothe-Satney and Yang et al., 2000; Gingras and Raught et al., 2001) (see Figure 1.3). 4E-BP1 is phosphorylated in a hierarchical manner: the N-terminal sites, Thr46 and Thr37, are the "priming sites" that need to be phosphorylated before Thr70 and Ser65 can be acted upon. Thr70 and Ser65 are adjacent to the eIF4E-binding motif and their phosphorylation directly regulate binding to eIF4E (Gingras and Gygi et al., 1999). Ser101 is constitutively phosphorylated and is required for the phosphorylation of Ser65 (Wang and Li et al., 2003).

Two important regulatory motifs have been identified in 4E-BP1. The C-terminal TOS (TOR-signalling) motif allows 4E-BP1 to bind the raptor component of mTORC1 and leads to phosphorylation (Beugnet and Wang et al., 2003; Choi and McMahon et al., 2003; Nojima and Tokunaga et al., 2003; Schalm and Fingar et al., 2003). Mutating the TOS motif impairs the phosphorylation of Ser101, Thr70 and Ser65 on 4E-BP1 (Beugnet and Wang et al., 2003). The N-terminal RAIP (amino acid sequence) motif plays a role in the phosphorylation of additional sites (Beugnet and Wang et al., 2003) and this motif is shared by other targets of mTOR: the ribosomal S6 kinase 1/2 (Schalm and Blenis, 2002; Fonseca and Smith et al., 2007).

While many intracellular signalling pathways have been implicated in modulating 4E-BP1 phosphorylation, mTOR (mammalian target of rapamycin) signalling seems to be

the final conveyor involved in 4E-BP1 regulation (Gingras and Raught et al., 1999). In response to insulin or phenylephrine in adult rat ventricular cardiomyocytes (Wang and Wang et al., 2000; Wang and Proud, 2002), 4E-BP1 undergoes phosphorylation and is released from eIF4E allowing the formation of eIF4F complexes. The phosphorylation of 4E-BP1 *in vivo* is inhibited by rapamycin showing a key role for mTOR signalling in this event (Wang and Wang et al., 2000; Wang and Proud, 2002). This observation is not limited to cardiomyocytes. Embryonic stem (ES) cells which have been depleted of mTOR show decreased phosphorylation of 4E-BP1 at Thr37, Thr46, Thr70, and Ser 65 (Wang and Beugnet et al., 2005), showing that mTOR is essential for the phosphorylation of 4E-BP1. In fact, mTOR has been shown to phosphorylate 4E-BP1 *in vitro* (Brunn and Hudson et al., 1997; Burnett and Barrow et al., 1998). Although it was initially suggested that mTOR phosphorylates only the priming sites (Thr37/46), subsequent studies showed that Ser65 and Thr70 display higher sensitivity to rapamycin, implicating a more critical role for mTOR in the regulation of 4E-BP1 and eIF4F function (Gingras and Gygi et al., 1999; Gingras and Raught et al., 2001).

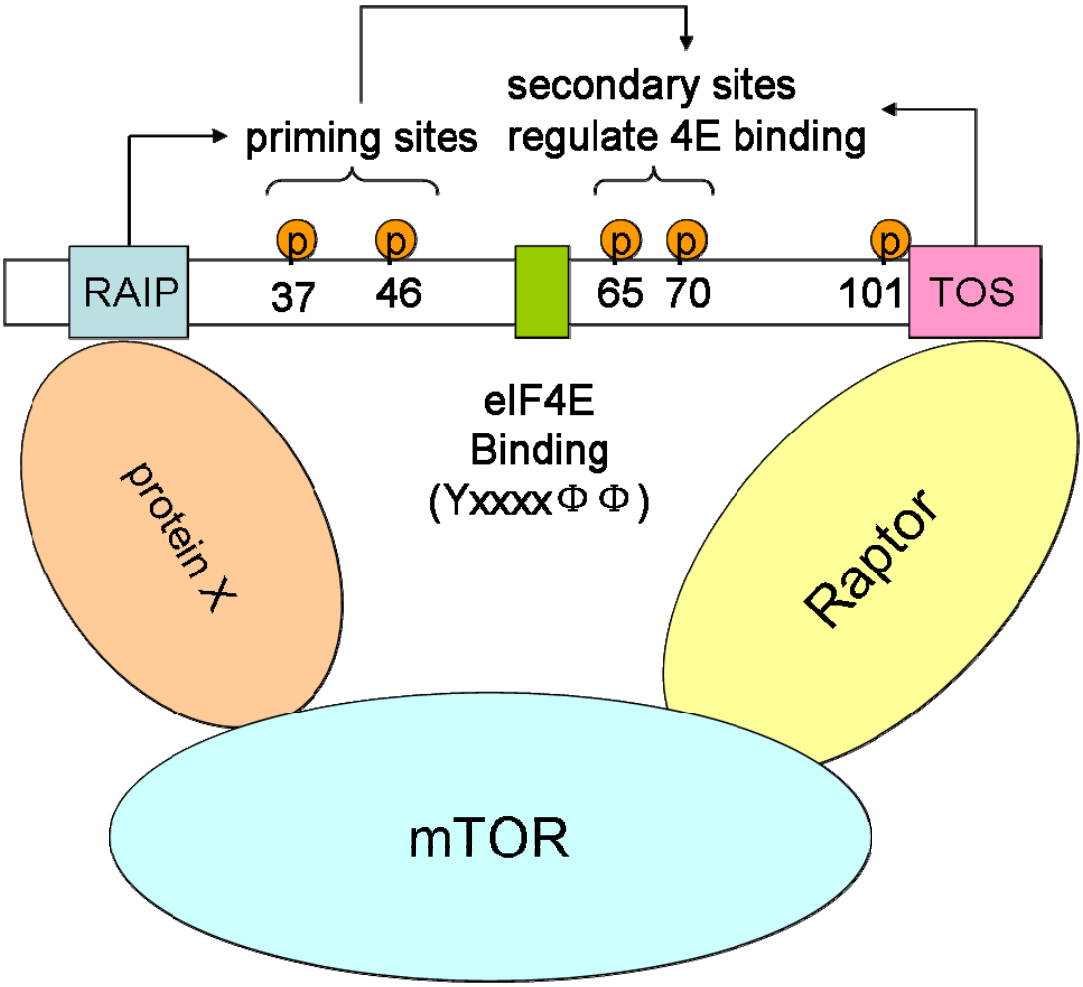

FIGURE 1.3. Diagram depicting a current model for the phosphorylation of 4E-BP1. The 4E-BP1 protein is phosphorylated in a hierarchical manner. Thr46 and Thr37 are the priming sites that need to be phosphorylated before the secondary sites, Thr70 and Ser65, can be phosphorylated. The secondary sites regulate eIF4E-affinity of 4E-BP1 as they are in proximity with the eIF4E-binding motif (green box). mTOR is essential for the phosphorylation of Thr37, Thr46, Ser65and Thr70. The latter two phosphorylation events depend on the interaction between the raptor component of mTORC1 and the TOS motif (pink box) of 4E-BP1 (denoted by arrow). The hypothetical "protein X" represents an unknown binding partner for the RAIP motif. Raptor has also been shown to interact with the RAIP motif (Lee and Healy et al., 2008), which has been proposed to mediate the phosphorylation of Thr37 and Thr46 (denoted by arrow).

1.4 Rapamycin and its target: the mammalian target of rapamycin (mTOR)

mTOR is a huge multi-domain protein (289 kDa). One of its domains resembles the kinase domain of the members of the phosphatidylinositide kinase family. However, mTOR does not possess lipid kinase activity and has actually been shown to act as a serine/threonine protein kinase (Keith and Schreiber, 1995; Hoekstra, 1997; Thomas and Hall, 1997). As its name suggests, mTOR is highly sensitive to inhibition by the immunosuppressant rapamycin, which suppresses mTOR activity by binding to a small and highly conserved immunophilin FKBP12 (FK-506 binding protein 12). The rapamycin-FKBP12 complex then specifically binds to the FRB (FKBP12/rapamycin binding) domain of mTOR adjacent to its kinase domain. The FRB domain is absolutely essential for rapamycin to inhibit mTOR because a single point mutation within the domain disrupts the binding of rapamycin-FKBP12 to mTOR and leaves mTOR active to phosphorylate its substrate (Brown and Beal et al., 1995). This suggests that binding of rapamycin-FKBP12 to the FRB domain suppresses mTOR catalytic activity. However, it is not entirely clear exactly how rapamycin inhibits mTOR and there are evidence showing that some functions of mTOR are insensitive to rapamycin (Fingar and Blenis, 2004). In fact, mTOR exists as two distinct complexes, mTORC (mTOR complex) 1 and mTORC2. Several features, including molecular composition and cellular roles in different processes, distinguish mTORC1 from mTORC2. Most important of all is the observation that rapamycin only efficiently inhibits the function of mTORC1 while mTORC2 remains largely insensitive to it (Sarbassov and Ali et al., 2006). Consistently,

rapamycin-FKBP12 only interacts with mTORC1 (Jacinto and Loewith et al., 2004; Sarbassov and Ali et al., 2004). In the context of protein synthesis regulation, this present study focuses on mTORC1 since its best-studied targets, including 4E-BP1 and S6Ks (p70 ribosomal S6 kinses), could directly modulate protein synthesis (Averous and Proud, 2006).

1.5 mTOR, protein synthesis, and cell growth

Accumulating evidence, such as genetic analysis in *Drosophila*, suggests that mTORC1 signalling plays a key role in cell and animal growth (Thomas and Hall, 1997; Zhang and Stallock et al., 2000; Fingar and Blenis, 2004). Inactivating mutations of the *Drosophila* TOR give rise to flies of smaller sizes than the wild type (Oldham and Montagne et al., 2000; Zhang and Stallock et al., 2000). Similarly, inhibition of mTORC1 by rapamycin leads to marked reduction in mammalian cell size (Schmelzle and Hall, 2000). Given that cardiac hypertrophy involves increased cell size, these observations suggest mTOR may play a role in the development of cardiac hypertrophy. In adult rat ventricular cardiomyocytes, the stimulation of protein synthesis by insulin or by the hypertrophic agonist PE is largely inhibited by rapamycin (Wang and Wang et al., 2000; Wang and Proud, 2002). Most importantly, mTORC1 was strongly implicated in the development of cardiac hypertrophy when rapamycin was reported to attenuate and/or even reverse cardiac hypertrophy in mice (Shioi and McMullen et al., 2003; McMullen

and Sherwood et al., 2004). The link between mTORC1 and protein synthesis and cell growth is likely its downstream effectors, S6Ks and 4E-BPs. Each of these proteins has also been implicated in the regulation of protein synthesis and cell growth.

Knocking out the single *ds6k* gene in *Drosophila* results in a severe reduction in body size due to smaller cell size, but not cell number (Montagne and Stewart et al., 1999). The size reduction of cells from these S6K-deficient fruit flies may be a direct result of slower growth rate. Similar experiments were performed in mammalian systems where the two homologous *S6k* genes, *s6k1* and *s6k2*, are knocked out. Consistent with the findings in *Drosophila*, transgenic mice ($S6k1^{-/-}$) that lack S6K1 activity are smaller in whole animal size than their wild type counterpart (Shima and Pende et al., 1998) due to defective cell growth rather than cell proliferation. However, deletion of *S6k2* gene in mice leads to mice that are slightly larger (Pende and Um et al., 2004). The different substrate specificity of S6K1 and S6K2 may account for the different phenotype observed. Surprisingly, in view of these data, the S6Ks are not required for cardiac hypertrophy in mice (McMullen and Shioi et al., 2004). Mice lacking S6K1 and S6K2 developed hypertrophy to similar extents as the wild type animals in response to aortic constriction (pathological hypertrophy), exercise (physiological hypertrophy) or treatment with growth agonists, like IGF-1. S6K signalling was thought to influence cell growth by regulating ribosome biogenesis (Ruvinsky and Meyuhas, 2006). However, this view has been largely discredited due to the observation that ribosome biogenesis proceeds normally in S6K-deficient animals (Shima and Pende et al., 1998; Tang and Hornstein et

al., 2001; Pende and Um et al., 2004; Hamilton and Stoneley et al., 2006).

It therefore seems that rapamycin-sensitive (mTORC1-regulated) events other than the S6 kinases serve to mediate the development of cardiac hypertrophy. Compelling evidence suggests that the other well-studied mTORC1 target, 4E-BPs, are also involved in the control of cell growth. Ectopic expression of a highly active mutant form of *Drosophila* 4E-BP in wing imaginal discs leads to a reduction of wing size, which is caused by a decrease in both cell size and cell number (Miron and Verdu et al., 2001). Similarly, mice lacking both 4E-BP1 and 4E-BP2 gain more weight than the wildtype mice when they are both fed in a high-fat diet (Le and Petroulakis et al., 2007). These findings are consistent with 4E-BP's inhibitory role in the regulation of protein synthesis (refer to section 1.3). The increase in body weight was mostly due to increases in fat accumulation in several tissues and organs, especially adipose tissue and the liver. The accumulation of fat in the 4E-BP1/4E-BP2 double-knockout mice was accompanied by an increase in adipocyte size, but again there was no significant increase in adipocyte number. All in all, the above evidence suggests that 4E-BPs primarily regulate cell growth, but not proliferation.

1.6 TSC1/2 complex – a negative regulator of mTORC1 signalling

Loss-of-function mutations in the genes for TSC1 (tuberous sclerosis 1, also known as hamartin) and TSC2 (tuberous sclerosis 2, also referred to as tuberin) give rise to a

condition termed tuberous sclerosis (TSC). It is an autosomal dominant disorder in which patients develop benign tumors (hamartomas) characterized by very large cell size (Cheadle and Reeve et al., 2000). Indeed, giant cells are a hallmark of hamartomas, suggesting that TSC1 and TSC2 most likely participate in the negative regulation of cell growth (Cheadle and Reeve et al., 2000). Direct evidence supporting this claim was provided by *Drosophila* studies. It was shown that *Drosophila* cells lacking dTSC2 showed abnormal increase in cell size (Ito and Rubin, 1999). Similarly, disruption of *dTSC1* gene resulted in enhanced organ growth. Conversely, co-expression of dTSC1 and dTSC2 proteins leads to a dramatic reduction in cell and organ size (Gao and Pan, 2001; Potter and Huang et al., 2001). These connections between TSC1/2 and cell growth intrigued several researchers to investigate the relationship between these proteins and mTORC1 signalling, which is believed to play a central role in cell growth regulation. The first evidence for a solid connection between TSC1/2 and mTORC1 signalling comes from a *Drosophila* study which demonstrated that dTSC1 and dTSC2 inhibit cell growth by acting upstream of dS6K, which is an mTORC1 signalling target (Potter and Huang et al., 2001; Radimerski and Montagne et al., 2002). It was shown that dTSC1 physically interacts with dTSC2 and together functions as a complex to inhibit the activation of dS6K (Radimerski and Montagne et al., 2002). Biochemical and genetic data indicate that in mammalian cells TSC1/2 complex functions upstream of mTORC1 to negatively regulate signalling downstream (Manning and Tee et al., 2002; Tee and Fingar et al., 2002).

TSC2 (around 200 kDa) has a GAP (GTPase activating protein) domain that catalyzes the hydrolysis of GTP to GDP in small G-proteins. TSC1, the less-studied partner of TSC2, is around 130 kDa and is thought to function as a scaffolding protein that stabilizes TSC2 by forming a complex with it in the cell (Tee and Fingar et al., 2002). Co-expression of TSC1 and TSC2 in mammalian cells partially inhibits the insulin-induced phosphorylation of S6K1 and 4E-BP1, consistent with earlier findings in *Drosophila* that dTSC1/2 complex negatively regulates signalling downstream of mTORC1 (Manning and Tee et al., 2002; Tee and Fingar et al., 2002).

The observation that TSC2 is a GAP suggests that a G-protein most likely relays the signals from TSC1/2 complex to mTORC1 signalling and cell growth. dRheb (*Drosophila* Ras homologue enriched in brain) was identified as the downstream target of the tuberous sclerosis complex by several independent groups (Saucedo and Gao et al., 2003; Stocker and Radimerski et al., 2003; Zhang and Gao et al., 2003). Rheb is a member of the Ras superfamily GTPases and is homologous to Ras. GTPases are active in their GTP-bound state and inactive in the GDP-liganded form. Mutation of Ser20 (a highly conserved residue required for Ras activity (Feig and Cooper, 1988) in Rheb abolishes its binding to both GTP and GDP (Li and Inoki et al., 2004). Such a Rheb mutant fails to activate mTORC1 signalling presumably because it cannot be activated by GTP binding (Li and Inoki et al., 2004; Drutskaya and Ortiz et al., 2005). Conversely, mutation of Gln64 to leucine in Rheb results in prolonged GTP binding (Li and Inoki et al., 2004) as this residue corresponds to a conserved residue in Ras that is required for

efficient GTP hydrolysis (Scheffzek and Ahmadian et al., 1997). Notably, Rheb[Gln64Leu] is more efficient than wild type Rheb at stimulating mTORC1 signalling (Inoki and Li et al., 2003). By interacting with mTORC1, GTP-Rheb stimulates mTOR kinase activity *in vitro* (Long and Ortiz-Vega et al., 2005). Together these data indicate that Rheb switches on mTORC1 signalling and its activity is regulated by GTP binding.

In mammalian cells, depletion of Rheb by small interfering RNA decreases cell size (Findlay and Yan et al., 2007), consistent with a positive role for Rheb in the control of cell growth. Conversely, targeted overexpression of dRheb in the *Drosophila* eye increases the size of the ommatidia (the eye unit) (Saucedo and Gao et al., 2003). The augmented growth caused by overexpression of dRheb in the eye was reversed by simultaneous deletion of the *dS6k* gene indicating that dRheb functions upstream of dS6K (Saucedo and Gao et al., 2003). Indeed, Rheb is a direct target for TSC1/2 regulation. TSC1/2 activates the intrinsic GTPase activity of Rheb *in vitro*, suggesting that TSC1 and TSC2 together function as a GTPase-activating protein for Rheb *in vivo* (Tee and Manning et al., 2003). Consistently, overexpression of Rheb in adult ventricular cardiomyocytes also causes an activation of mTORC1 signalling and an increase in cell size (Wang, 2008 unpublished).

1.7 The classical MEK/ERK pathway and mTORC1 signalling

Although PI3K, PKB/Akt, and mTORC1 signalling plays a dominant and central role in the modulation of 4E-BP1 phosphorylation in most cell lines tested so far in response to insulin and growth factors (Wang and Proud, 2006), growing evidence suggests that other signalling pathways, such as the Mitogen-activated protein (MAP) kinase (MAPK) pathways, may function in a co-regulatory capacity or may participate in a "cross-talk" with the mTORC1 signalling pathway to regulate cell growth, division and differentiation. The MAP kinase cascade includes a MAP kinase (e.g. Erk), an upstream MAP kinase kinase (e.g. MEK) and a MAP kinase kinase kinase, such as Raf, which is in turn activated by Ras, a small G-protein (Kolch, 2000) (see Figure 1.4). The MAP kinases are a large family of widely expressed protein Ser/Thr kinases (Cohen, 1996). The present study focuses on the role of extracellular signal-regulated kinases (Erks) in the classical MEK/Erk pathway in the control of protein synthesis and the development of cardiac hypertrophy.

Numerous studies have proposed that the classical MEK/Erk cascade is involved in the cardiac hypertrophic response. Initially, some studies showed that, in response to agonist stimulation or cell stretching, Erk1 and 2 become activated either in cultured cardiac myocytes and in isolated perfused hearts (Yamazaki and Tobe et al., 1993; Clerk and Bogoyevitch et al., 1994; Bogoyevitch and Gillespie-Brown et al., 1996; Lazou and Sugden et al., 1998). In support of this notion, the re-expression of neonatal genes, another feature of cardiac hypertrophy, can be induced by transfection of a constitutively

active MEK1-encoding construct (immediate upstream activator of Erk1 and 2) whereas a dominant-negative MEK1-encoding construct inhibits it (Gillespie-Brown and Fuller et al., 1995). Using antisense oligonucleotides, it was demonstrated that Erk signalling is necessary for PE-induced cardiomyocyte hypertrophy in culture (Glennon and Kaddoura et al., 1996). In a more recent study, a series of transgenic mice were generated expressing an activated mutant of MEK1 in the heart. Expression of activated MEK1 in the mouse heart promoted specific activation of Erk1/2, which was associated with a long-standing physiologic hypertrophic response characterized by increased cardiac function and partial resistance to apoptotic stimuli (Bueno and De et al., 2000). These evidences firmly establish the MEK/ERK signalling pathway as a hypertrophic mediator *in vivo*.

Cardiomyocytes are terminally-differentiated cells. In these cells, adaptive hypertrophic growth involves increases in protein content, cell size, myofibrillar organization, and changes in gene expression (Proud, 2004). PE, an α1-adrenergic agonist that acts through Gq-protein-coupled receptors (GPCR), exerts hypertrophic effects and stimulates protein synthesis in cardiomyocytes (Clerk and Sugden, 1999; Molkentin and Dorn, 2001). There is substantial evidence that the activation of protein synthesis requires the MEK/Erk signalling cascade (Bogoyevitch and Glennon et al., 1994; Clerk and Sugden, 1999; Bueno and De et al., 2000; Yue and Gu et al., 2000). Hypertrophic agonists, such as PE, acutely activate MEK/Erk signalling and induce protein synthesis in adult rat ventricular cardiomyocyte and this effect is blocked by inhibitors that target

MEK, such as PD098059, PD184352, U0126 (Wang and Gout et al., 2001; Wang and Proud, 2002; Wang and Proud, 2002). In ARVC, PE was also found to regulate several components of the translational machinery, such as activation of S6k1, phosphorylation of 4E-BP1, formation of eIF4F complexes and the dephosphorylation of eEF2, in a MEK-dependent manner. These events are most likely not direct effects of MEK itself on these proteins since MEK is highly specific for Erk but more likely reflects a role for Erk, or kinases downstream of Erk, such as $p90^{RSKs}$ (p90 ribosomal protein S6 kinases). In fact, it was shown that Erk is required for the upregulation of mTORC1 (Rolfe and McLeod et al., 2005). These are strong evidence that MEK/Erk signalling controls mTORC1 activity.

By analogy with the regulation of mTOR by PI3K/PKB signalling, it is likely that the stimulation of MEK/Erk signalling results in phosphorylation and inactivation of TSC2, allowing GTP-Rheb to accumulate and turn on mTORC1 signalling. However, it is unclear how the MEK/Erk pathway regulates TSC1/2 and thus mTORC1. One report suggests that this involves direct phosphorylation of TSC2 by Erk (Ma and Chen et al., 2005), while others indicate that TSC2 is phosphorylated by the $p90^{RSKs}$, enzymes that are activated directly by Erk (Roux and Ballif et al., 2004; Ballif and Roux et al., 2005; Rolfe and McLeod et al., 2005). $p90^{RSKs}$ appear to phosphorylate TSC2 at sites that are distinct from those targeted by PKB. Phosphospecific antibodies are available for the PKB sites in TSC2. However, PE does not increase the phosphorylation of these sites in ARVC but instead enhances the phosphorylation of distinct sites as detected with a different antiserum designed to recognize phosphorylation of residues within the

consensus RXRXXpS/pT, where pS and pT are phosphoserine or phosphothreonine (Roux and Ballif et al., 2004; Rolfe and McLeod et al., 2005). This phosphorylation is blocked by the MEK inhibitor U0126 and also by two other MEK inhibitors (PD098059/PD184352) (Rolfe and McLeod et al., 2005). $p90^{RSKs}$ lie downstream of Erk and have sequence specificity which matches the above type of motif. Hence, how the MEK/Erk pathway regulates mTORC1 signalling through the phosphorylation of TSC1/2 complex remains a critical question to be solved.

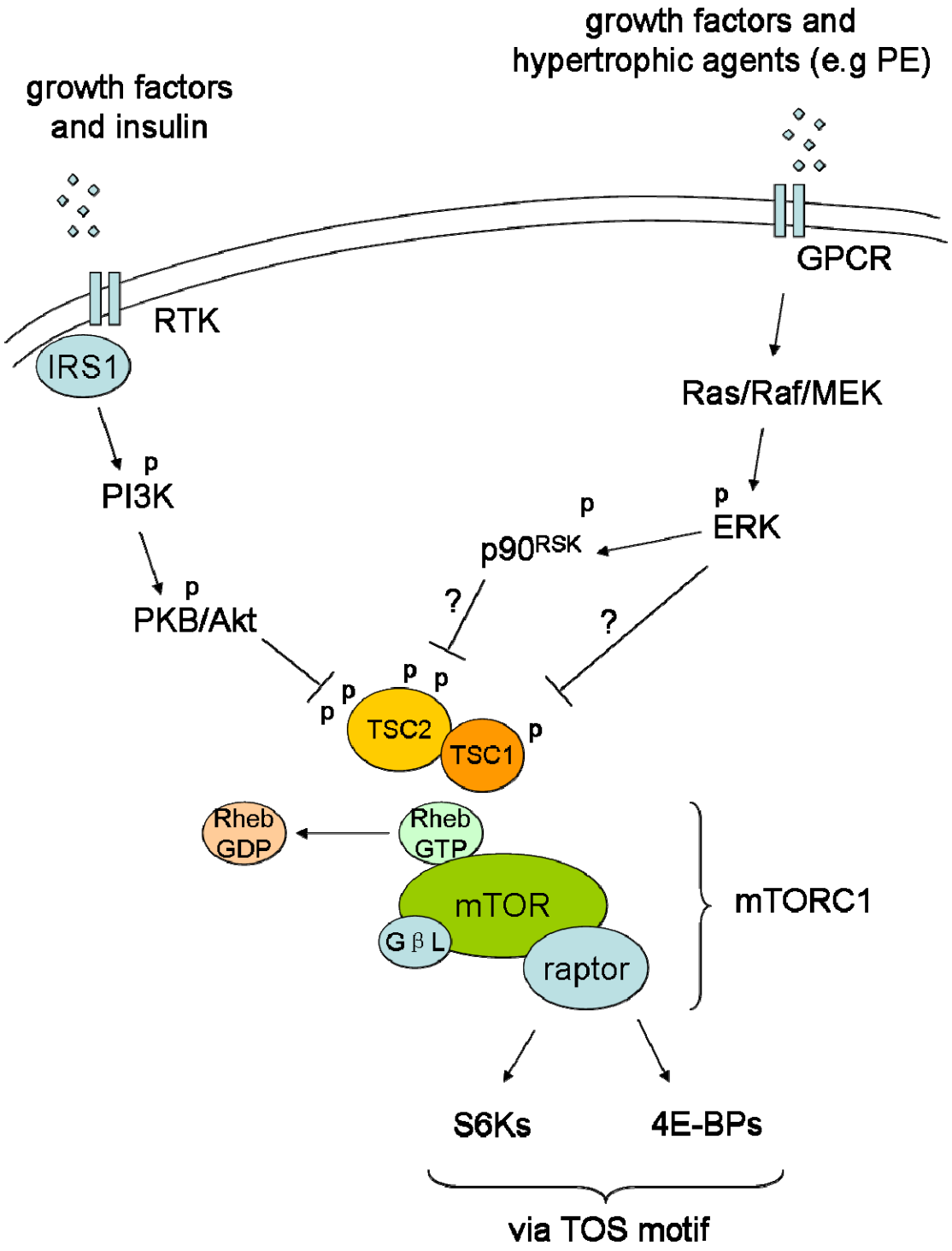

FIGURE 1.4. The current model of mTORC1 signalling and its upstream regulation. Insulin binds to the receptor tyrosine kinase (RTK) to induce activation of PI3K, which indirectly leads to the phosphorylation and activation of PKB/Akt. Active PKB/Akt phosphorylates and inactivates TSC2 allowing active Rheb (GTP-bound) to accumulate and switches on mTORC1 signalling. Through the interaction between raptor and the

TOS motif on its substrates, mTOR is thought to directly phosphorylate 4E-BPs and S6Ks. Hypertrophic agents, such as PE, act through the classical MEK/Erk signalling pathway to phosphorylate TSC2 at distinct sites from those of the PI3K/PKB pathway and inactivates TSC1/2 complex to turn on mTORC1. It is currently unclear which downstream kinase(s) of the MEK/Erk pathway is responsible for the phosphorylation of TSC2. Current literature suggest that it could be Erk itself or by its downstream effector $p90^{RSKs}$. "p" denotes phosphorylation.

1.8 Aims of this study

The current literature supports the idea that mTORC1 signalling plays a central role in cell growth and most likely participates in the development of cardiac hypertrophy. This study therefore aimed (i) to characterize the functional significance of mTORC1 signalling target, 4E-BP1, in the context of the control of protein synthesis and cell growth in adult rat ventricular cardiomyocytes, and (ii) to investigate how the classical MEK/Erk pathway regulates mTORC1 signalling through the TSC1/2 complex in response to PE. By studying signalling both upstream and downstream of mTORC1 in this project, I am hoping to gain further knowledge at the molecular level about how PE induces protein synthesis and thus the development of cardiac hypertrophy, focusing especially on how TSC1/2 complex is deactivated by phosphorylation and the role of 4E-BP1/eIF4F.

Chapter 2

Materials and Methods

2.1: Chemicals and biochemicals

All chemicals and biochemicals were obtained from Sigma-Aldrich unless otherwise stated. [γ-^{32}P]ATP, L-[^{35}S]methionine, m^{7}GTP-Sepharose CL-4B, and enhanced chemiluminescence (ECL) reagents were purchased from Amersham Pharmacia Biotech. Protein G-Sepharose was bought from GE Healthcare. pRK7-FLAG-TSC1 and pRK7-FLAG-TSC2 vectors were generous gifts from Dr. Andrew Tee (Cardiff, UK). Anti-eIF4G and anti-4E-BP1 antibodies were kindly provided by Dr. Simon Morley (Sussex, UK) and Dr. A. Thomas (Utrecht, The Netherlands), respectively. Luciferase substrate (Promega) was acquired from Fisher Scientific. PD098059 and rapamycin were supplied by Calbiochem. BI-D1870 was obtained from the Division of Signal Transduction Therapy of the University of Dundee. Bovine serum albumin (BSA, fraction V) was from Roche Molecular Biochemicals. Collagenase (type II) was purchased from Worthington Biochemical. Tissue culture reagents were provided by Invitrogen. X-Omat^{TM} Blue XB-1 film was purchased from Kodak Scientific Imaging. Immobilon-PVDF transfer membrane of 0.45 μm pore size was from Millipore. 3MM filter paper was from Whatman International. Bradford reagent was from Bio-Rad Laboratories. Nylon monofilament filter cloth (200 μm) was purchased from Cadisch Precision Meshes. Dialysis tubing of size 5 (MWCO: 12-14000 Da) was from Medicell International. Econofluor scintillation liquid was from Packard Instruments. Activated human Erk1 was purchased from Cell Signaling.

2.2: Adult rat ventricular cardiomyocyte (ARVC) retrograde perfusion

2.2.1 Isolation of ventricular cardiomyocytes from adult male *Rattus norvegicus*

Adult rat ventricular cardiomyocytes (ARVC) were prepared from adult male Sprague-Dawley rats (250-300 g; Animal Care Center, UBC) by collagenase perfusion (Wang and Proud, 2002). Given the sensitive nature of the cardiomyocytes, an efficient isolation procedure which minimizes stress and damage to the cells is essential for subsequent successful cell culture and experiment reproducibility. The survival of cardiomyocytes in culture is highly dependent on the quality of the isolation.

All solutions involved in the cardiomyocyte isolation were prepared with Milli-Q Ultrapure H_2O. The stock Ca^{2+}-free buffer (see Table 1) serves as a base cocktail for the making of the five main solutions used during the isolation. It is important to note that the pH of the stock Ca^{2+}-free buffer must be adjusted with concentrated NaOH to about 7.25 to 7.30 prior to use.

TABLE 1.1. Composition of the stock Ca^{2+}-free buffer.

Chemical	Conc. [mM]	for 1000ml
NaCl	130	7.9g
HEPES	5	1.19g
D-Glucose	10	1.8g
KCl	5.4	0.336g
$MgCl_2 \cdot 6H_2O$	3.5	0.712g
NaH_2PO_4	0.4	0.062g

1. 750 μM Ca^{2+} solution:
200 ml Ca^{2+}-free buffer + 150 μl 1M $CaCl_2$

2. 100 μM EGTA solution:
100 ml Ca^{2+}-free buffer + 100 μl 100mM EGTA

3. Enzyme solution (1 mg/ml collagenase, 90 μM Ca^{2+}):
50 ml Ca^{2+}-free buffer + 50 mg collagenase (type II) + 4.5 μl 1M $CaCl_2$

4. Wash Solution:
90ml Ca^{2+}-free buffer + 10 μl 1M $CaCl_2$ + 10ml 10% BSA

5. Heparin Beaker Solution:
25 ml Ca^{2+}-free buffer + 18.5 μl 1M $CaCl_2$ + 60 μl 5000 unit/ml Heparin

BSA powder was dissolved in modified Ca^{2+}-free buffer (containing 80 μM Ca^{2+}) to a concentration of 100 mg/ml under constant stirring at 4ºC. The dissolved BSA mixture was then subjected to dialysis against the modified Ca^{2+}-free buffer (containing 80 μM Ca^{2+}) for 1 h at 4 ºC and then was further dialysed against fresh modified Ca^{2+}-free buffer (containing 80 μM Ca^{2+}) overnight at 4 ºC. The dialysed BSA solution was aliquoted and stored under -20ºC. No significant difference was found in cell behavior with fatty acid present in the BSA preparation.

The heart weighs about 0.4% of the whole body in 250 g rats. Experience indicates that, 9 ml/min per gram of heart is optimal for retrograde perfusion. Therefore, the following calculations are followed to determine the perfusion rate:

Animal weight X (g) x 0.4 % = heart weight Y (g)

Heart weight Y (g) x 9 ml/min,g = Z ml/min = perfusion rate for a heart of weight X (g)

Before the perfusion, all solutions were prewarmed to 37ºC and oxygenated for at least 5 min. Adult rats were sacrificed by stunning and cervical dislocation. After opening the thoracic cavity, the heart with the aorta still intact was swiftly excised and immersed in the "Heparin Beaker solution" to prevent clotting in the coronary vessels, which are the main routes for the retrograde perfusion. The heart was gently compressed 2 to 3 times to expel any residual blood. Immediately, the heart was tied to the tip of the cannula through the aorta by surgical silk and the perfusion began. The heart was perfused with the "750 μM Ca^{2+} solution" for 2 min to flush away any remaining blood, "100 μM EGTA solution" for 4 min to stop contraction, and then the "enzyme solution" for 18 to 20 min to digest away the collagenous extracellular matrices. During the enzyme digestion, collagenase was recollected and recirculated for the perfusion and subsequent digestion. After the enzyme perfusion, the heart was removed from the cannula and excess fat and connective tissue was trimmed away. The remaining ventricular muscle tissue was cut into several pieces to facilitate exposure to collagenase. The ventricular tissue then underwent 3 to 4 rounds of mechanical separation in which the tissue was further digested with 5 ml of the oxygenated enzyme solution containing 1% BSA in a 50-ml flat bottom flask under mild shaking at 37ºC for 5 min. After each round of digestion, dislodged cardiomyocytes were separated from undigested tissue by filtration through a nylon filter cloth (200 μm). The isolated cardiomyocytes were washed by the "wash solution" and allowed to sediment under gravitation for 3 times to remove the non-myocytes and the damaged and dead myocytes.

The remaining cells were further washed by low glucose DMEM with 1.0 mM EGTA for 2 times and M199 (Medium 199) with 1.0 mM EGTA for 2 times. Finally, the cells were resuspended in modified tissue culture M199 (2 mM glutamine, 50 U/ml penicillin, 50 ug/ml streptomycin, 5 mM creatine, 2 mM carnitine, 5 mM taurine, 1.0 mM EGTA) prior to tissue culture. Normally a successful cardiomyocyte isolation will have a 95% yield of healthy living rod-shaped cardiomyocytes.

2.2.2 Tissue Culture of adult rat cardiomyocytes

Six-well flat bottom plates (Becton Dickinson Labware) and 60 mm dishes (Techno Plastic Products) of tissue culture grade were precoated with laminin, which provides an artificial matrix for the isolated cardiomyocytes to adhere to. The coating process involves incubating the tissue culture dishes with M199-diluted laminin (10 μg/ml) at room temperature for at least 30 min. Care was taken to ensure that all surfaces were sufficiently covered by laminin. The coating mixture was then removed by aspiration and excess laminin was rinsed away by M199 medium. The coated tissue culture dishes were supplied with modified tissue culture M199 medium and were allowed to equilibrate in a 37 ºC incubator (5% CO_2) for at least 30 min.

Cardiomyocytes were seeded roughly at a density of 1.57 x 10^4 cells/cm^2 and were allowed to adhere to the tissue culture dishes for 2 h. Non-attached cells were removed after the 2-h incubation by aspiration. Fresh modified M199 medium was replenished to

the adherent healthy rod-shaped cardiomyocytes and they were immediately infected with adenovirus as described below or incubated without infection overnight before any further treatments. If long term culture is required, cardiomyocytes have been maintained and closely monitored for at least five days after their isolation. The cells generally exhibit normal morphology with no aberrant signalling activity. However, cardiomyocyte culture has been limited to two to three days to ensure consistency in the quality of the cardiomyocytes.

2.2.3 Cell treatment and protein extraction

Cells were treated with signalling inhibitors and agonists after at least a 16-h overnight culture or longer (40 h) in cases when adenoviruses had been employed to mediate gene transfer. The final concentrations of the signalling inhibitors in this study were: Rapamycin 100 nM; PD98059 50 μM; BI-D1870 5, 10, or 20 μM. The signalling inhibitors were diluted with the culture medium immediately before addition to the cell culture to prevent precipitation and ensure equal distribution throughout the tissue culture dish. After a certain inhibition period which depends upon the experiments taking place, cells were treated with or without agonists such as PE (10 μM). Again, the stimulation time differed between types of experiments and will be stated in the corresponding sections. Rapamycin disrupts mTORC1 signalling (Wang and Proud, 2002). PD98059 targets MEK (Wang and Proud, 2002). BI-D1870 is a specific $p90^{RSKs}$ inhibitor (Sapkota

and Cummings et al., 2007).

After treatment, tissue culture dishes were placed on ice. Medium was removed by aspiration and the cells were washed twice with ice-cold PBS (phosphate-buffered saline: 2 mM KH_2PO_4 pH 7.4, 10 mM Na_2HPO_4, 4 mM KCl, 170 mM NaCl). Sufficient volume of protein extraction buffer (50 mM Tris pH 7.5, 1 mM EGTA, 1 mM EDTA, 1mM Na_3VO_4, 50 mM NaF, 5 mM sodium pyrophosphate, 1% (v/v) Triton X-100, 1 mM DTT, 1 μg/ml leupeptin, 1 μg/ml pepstatin, 1 μg/ml antipain, and 0.2 mM PMSF) was added and cells were lysed mechanically by scraping. Membrane debris, mitochondria, and nuclei were spun down (16.1 *r.c.f.*) for 10 min at 4ºC and discarded as pellets. The supernatant was collected for subsequent analysis.

2.2.4 Adenovirus-mediated gene transfer

The recombinant adenoviruses encoding luciferase B0 and B4 were kind gifts from Dr. Paul McDermott (Tuxworth and Saghir et al., 2004). The other adenoviruses (GFP, LacZ, 4E-BP1 wildtype and LM/AA mutant form) used in this study were constructed and prepared by Dr. Yanni Wang.

Adenovirus-mediated gene transfer was performed after ARVC had attached to the laminin-coated tissue culture dishes (Wang and Proud, 2002). ARVC were incubated at 37˚C with recombinant adenoviruses in minimal volume of M199 medium for 2 to 3 h at the multiplicity of infection (m.o.i.) indicated in the figure legends. Fresh M199

medium was supplied to the cells after removing the virus. ARVC were cultured for a further 40 h to allow expression of the gene of interest before further treatment. Viruses encoding either the green fluorescent protein (GFP) or β-galactosidase (lacZ) were used as negative controls: the former allows the efficiency of transfection to be assessed readily, under the fluorescence microscope, while the latter was created using the same system as the other adenoviral vectors used here. In fact, neither virus had any effects on the parameters studied here, and they can therefore be used interchangeably.

2.3: Human embryonic kidney (HEK) 293 cell line

2.3.1 HEK293 cell culture

Human embryonic kidney (HEK) 293 cells (Division of Signal Transduction Therapy of the University of Dundee) were cultured on sterile 6-cm or 10-cm diameter plates (Nunc) in Dulbecco's Modified Eagle's Medium (DMEM) supplemented with 10% (v/v) fetal bovine serum (FBS) and 2 mM L-glutamine. Penicillin G and streptomycin sulphate were supplied to the medium at a final concentration of 100 units/ml and 100 μg/ml, respectively. Cells were cultured in a humidified incubator at 37˚C and 5% (v/v) CO_2. When cells reached 80% confluence, they were passaged: medium was removed by aspiration and cells were gently rinsed with 8 ml of prewarmed sterile PBS twice. Care should be taken during this washing step to prevent accidental removal of cells due to mechanical disturbance of the attached cells. PBS was then aspirated and 1 ml of 0.05%

(w/v) trypsin/EDTA was added to the culture dish and the cell detachment was allowed for 3 min at 37˚C. The culture dish was tapped gently to detach cells (the detached patches of cells should be visible) . Detached cells were resuspended to single cell suspension in growth medium and seeded in new sterile tissue culture dishes at the desired density.

2.3.2 Transient transfection of HEK293 cells by calcium-phosphate precipitation

HEK293 cells have phagocytic properties and readily take up DNA precipitated in a complex with calcium chloride. Cells were seeded at approximately 25% confluence and were allowed to attach to the tissue culture dishes for 7 h. Cells were then transfected with DNA by calcium-phosphate precipitation where plasmid DNA was precipitated by a solution containing 125 mM $CaCl_2$, 50 mM BES (N, N-bis [2-hydroxyethyl]-2 amino ethanosulphonic acid), 280 mM NaCl, and 1.5 mM NaH orthophosphate 2-hydrate. DNA-$CaCl_2$ precipitation complex is efficiently taken up by HEK293 cells into their cytoplasm and subsequently transferred to the nucleus. Cells were incubated with the DNA-calcium-phosphate precipitate for approximately 24 h, by which time the cells had reached 70% confluence. Transfection of HEK293 cells with this method gives invariably a transfection efficiency of up to 95%, as judged by GFP expression.

2.3.3 Cell treatment and protein extraction

Complete DMEM was removed by aspiration and HEK293 cells were rinsed once with prewarmed PBS. Cells were incubated with DMEM lacking fetal bovine serum for 16 h. After 16 h serum starvation, HEK293 cells were treated with the aforementioned MEK inhibitor PD098059 (50 μM) for 45 min before stimulation with phorbol 12-myristate 13-acetate (PMA, 1 μM) for 25 min. The cells were then harvested as described in section 2.2.3.

2.4: Protein Chemistry and biochemistry

2.4.1 Protein concentration determination

Concentration of the cell lysate was determined by the Bradford assay (Bradford, 1976) using the Bio-Rad Protein Assay Kit. The 5 x protein dye concentrate was diluted 5 times with distilled H_2O to make a 1 x Bradford reagent. One microlitre of cell lysate was mixed with 1 ml of the 1 x Bradford reagent in a 1-cm plastic cuvette. Content was mixed by inverting several times. The absorbance at 595 nm of the sample was then compared to a linear standard curve from serially diluted BSA (0 to 15 μg/μl) to estimate its concentration.

2.4.2 SDS-PAGE (sodium dodecyl sulphate polyacrylamide gel electrophoresis)

SDS-PAGE gels consisting of running gel: 10%, 12.5%, 13.5% (for 4E-BP1) acrylamide with 0.1% or 0.36% (for 4E-BPs) of N,N'-methylene-bis-acrylamide (both w/v) and stacking gel: 5% acrylamide with 0.13% N,N'-methylene-bis-acrylamide were polymerized by adding 10% (w/v) ammonium persulphate and TEMED. They were casted using Bio-Rad Mini Protean® III gel apparatus (Bio-Rad Laboratories). SDSPAGE was performed as previously described (Laemmli, 1970)in SDS-PAGE running buffer (384 mM glycine, 50 mM Tris and 0.1% (w/v) SDS) at 150 to 200 V. Prior to loading, protein samples were denatured by boiling with 5 x SDS sample buffer (0.5 M Tris-HCl pH 6.8, 10% (w/v) SDS, 20% (w/v) glycerol, 0.125% (w/v) bromophenol blue and 2 mM β-mercaptoethanol) for 5 min.

2.4.3 Electrotransferring and western blotting

After separation by SDS-PAGE, proteins were electrotransferred from SDSPAGE gels to Immobilon-PVDF (polyvinylidene fluoride 0.45 μm microporous membrane) in transfer buffer (192 mM glycine, 25 mM Tris and 0.02% (w/v) SDS, and 15% (v/v) methanol) using an Electro Blotting unit (Severn Biotech) for 1 h at 100 V as previously described (Lobert and Correia, 1994). The PVDF membrane was activated by methanol and equilibrated in transfer buffer prior to transfer. Generally, after the transfer, PVDF

membranes were blocked from non-specific binding by incubating with 5% (w/v) skim milk powder in PBS-Tween (PBS with 0.02% (v/v) Tween-20) for 1 h at room temperature under constant agitation. In the case when 4E-BPs were to be retained on the membrane, the membranes were fixed with 0.05% glutaraldehyde in 0.02% PBST for 20 min before blocking with milk protein. The blocked membranes were subsequently incubated with various primary antibodies (Table 2) diluted in 5% milk or 1% BSA in 0.02% PBST at 4 ºC overnight. After primary antibodies were removed and the membranes were washed 3 times with 0.02% PBST for 10 min, horseradish perioxidase conjugated secondary antibodies of mouse, rabbit, or sheep (Diagnostics Scotland) were allowed to react with the primary antibody on the membrane for 1 h at room temperature. After the secondary antibodies were discarded, the membranes were again washed 3 times with 0.02% PBST to remove unspecific binding. Enhanced Chemilumenescence (ECL) was applied to the membranes and the antigen-antibody complex was visualized upon exposure and development of X-ray films.

TABLE 1.2. Primary antibodies for western blot.

Antibody specificity	Species	Dilution	Source
anti-myc	mouse	1:2000	Sigma-Aldrich
anti-flag	mouse	1:2000	Sigma-Aldrich
anti-eIF4G	rabbit	1:1000	Dr. S. Morley (Sussex)
anti-eIF4E	rabbit	1:1000	Cell Signaling Technology
anti-eIF4E-BP1	rabbit	1:2000	Dr. A. Thomas (Utrecht)
anti-eIF4E-BP1 (p) Ser65	rabbit	1:1000	Cell Signaling Technology
anti-ERK	rabbit	1:1000	Cell Signaling Technology
anti-ERK (p) T202/Y204	rabbit	1:1000	Cell Signaling Technology
anti-ribosomal protein S6	rabbit	1:1000	Cell Signaling Technology
anti-ribosomal protein S6 (p) Ser235/236	rabbit	1:1000	Cell Signaling Technology
anti-ribosomal protein S6 (p) Ser240/244	rabbit	1:1000	Cell Signaling Technology
anti-eEF2	rabbit	1:1000	Dr. L.E. McLeod (Proud lab)
anti-eEF2 (p) Thr56	rabbit	1:1000	Dr. L.E. McLeod (Proud lab)
anti-TSC2 (C-20)	rabbit	1:500	Santa Cruz Biotechnology
anti-phospho-Akt-substrate	rabbit	1:1000	Cell Signaling Technology

2.4.4 m^7GTP Sepharose Chromatography

Affinity chromatography of eIF4E and associated proteins was conducted as follows: 15 µl of a 50/50 mixture of m^7GTP Sepharose CL-4B and Sepharose CL-4B were washed twice with standard extraction buffer and mixed with 200 µg of ARVC lysate. The mixture was rotated for 90 min at 4˚C. Subsequently, the affinity beads were pelleted by centrifugation (4.5× *g*, 15 s). Supernatants were removed by aspiration and the beads were washed three times in extraction buffer. Proteins were released from the beads by boiling in 5× SDS sample buffer at 95˚C for 5 min. SDS-PAGE and western blot procedures were carried out as described previously. Protein samples were resolved by SDS-PAGE and transferred onto PVDF membranes by electroblotting. Membranes were blocked with 5% (w/v) skimmed milk in 0.02% (v/v) PBS-Tween20™ for 60 min. The membranes were incubated overnight with the corresponding primary antibodies at 4˚C followed by horseradish peroxidase (HRP)-conjugated secondary antibodies for 60 min at room temperature. The membranes were developed by enhanced chemiluminescence (Amersham) on X-Omat™ Blue XB-1 film (Kodak).

2.4.5 TSC1 and TSC2 immunoprecipitation

To study endogenous TSC2 in ARVC and ectopically expressed TSC1 (flag tagged) in HEK293 cells, these proteins were enriched by immunoprecipitation. Thirty microliters of 80% Protein G-Sepharose beads were washed twice with ice-cold protein

extraction buffer and were preconjugated with anti-TSC2 antibody or anti-flag antibody at 4˚C for 1 h under constant rotation. Then, the antibody-bead complex was washed once with protein extraction buffer. One milligram of ARVC lysate or 500 µg of HEK293 cell lysate were further rotated for another 2 h at 4˚C. Subsequently, beads were collected by centrifugation (4.5 x *g*, 15 s). After the beads were washed twice with protein extraction buffer, the beads were stored at -80˚C for subsequent kinase assay or resuspended in 30 µl of 2 x SDS sample buffer and boiled at 95˚C for 5 min.

2.5: Analysis of cardiomyocyte hypertrophy

2.5.1 Measurement of general protein synthesis by L-[^{35}S]methionine incorporation

Fresh modified M199 medium was supplied to cultured ARVC 20 h before treatment with rapamycin (100 nM, 30 min). Cardiomyocytes were then stimulated with PE (10 µM, 45 min) prior to incubation with L-[^{35}S]methionine (5 µCi/ml) for another 45 min. After careful removal of the M199 medium, the cells were washed twice with ice-cold PBS and lysed with protein extraction buffer. Proteins were collected by filtration on 3MM filter paper (Whatman) before precipitation with 5% (w/v) cold trichloracetic acid (TCA) followed by boiling in the same solution for 5 min. Incorporated radioactivity was then measured using a MicroBeta Trilux liquid scintillation counter (Perkin Elmer).

Fresh modified M199 medium were supplied to overnight cultured (16 h) ARVC

20 h before treatment with rapamycin (100 nM, 30 min) where indicated. Following that, cells were treated with or without phenylephrine (10 μM, 45 min). Immediately after that, cells were then incubated with L-[^{35}S]methionine (5 μCi/mL) for an additional 45 min for *in vivo* labeling. After excess L-[^{35}S]methionine was removed along with the medium, cells were washed twice with ice-cold PBS and cell lysate was prepared as described in section 2.2.3. Eighty micrograms of proteins from each sample was collected by filtration on 3MM filter paper (2 cm x 2 cm) and precipitated in 5% (w/v) trichloracetic acid (TCA). Then, the filters were washed twice with boiling 5% (w/v) TCA (2 min each). Unincorporated L-[^{35}S]methionine was removed during this step. The filters were then quickly rinsed with 95% ethanol and dried in an oven of 100˚C for 20 min. Incorporated radioactivity was then measured using a MicroBeta Trilux liquid scintillation counter (Perkin Elmer).

2.5.2 Cell size measurement

After adenovirus infection, ARVC were treated with PE (10 μM, 40 h) or rapamycin (100 nM, 40 h) as indicated in the figure legends. After 40 h of incubation, 10× magnification images of the ARVC were taken by CoolSnap HQ^2 (Intelligent Imaging Innovations, Inc) using an inverted Zeiss 200M microscope. Cell area was estimated by tracing all living ARVC in a microscope field using Slidebook^{TM} 4.2 (Intelligent Imaging Innovations, Inc).

2.6: Analysis of translation regulation on specific mRNAs by Luciferase Assay

Cardiomyocytes were infected with LacZ or 4E-BP1 for 3 h after isolation. Sixteen h later, cells were infected with either luciferase B0 or B4 adenoviruses for 2 h. At the same time, cells were treated with 10 μM PE where indicated and were allowed to incubate at 37˚C overnight. Cells were rinsed three times in ice-cold PBS and lysed in reporter lysis buffer (Promega). Lysis was facilitated by scraping and quick freeze-thaw cycle at -80ºC. Preliminary luciferase assay was performed before each experiment to ensure the amount of luciferase in a reaction stayed within the linear range. Luciferase activity was measured by the Luciferase Assay System (Promega). Light emission was measured at room temperature by a Luminoskan Ascent luminometer (Labsystem). Luciferase activity was normalized to the total protein content in the reaction and the luciferase mRNA level, which was determined by qRT-PCR.

2.7: *In vitro* [^{32}P] radiolabelling of TSC1 and two-dimensional peptide mapping

2.7.1 *In vitro* [^{32}P] radiolabelling

HEK293 cells were transfected with 4.5 μg of DNA for FLAG-TSC1 and 5.0 μg for FLAG-TSC2. Twenty-four h after transfection, cells were serum starved for 16 h. After treatment as indicated in figure legends, cell lysates were prepared and FLAG-TSC1 and FLAG-TSC2 were immunoprecipitated. Beads with bound FLAG-TSC1 and FLAG-TSC2 were incubated with 30 μl of reaction mixture containing

5 mM MOPS, 2.5 mM β-glycerophosphate, 1 mM EGTA, 0.4 mM EDTA, 5 mM $MgCl_2$, 0.05 mM DTT, 100 μM ATP, 200 ng activated human ERK1, and 2.5 μCi [γ-^{32}P]ATP. Labelling reactions were incubated for 60 min at 30 ºC under constant agitation (1100 rpm) and terminated by adding 10 μl of 5x SDS sample buffer. SDS-PAGE was performed as described before and an X-ray film was exposed directly against the SDS-PAGE gel overnight. Purified human Mnk1 was kindly provided by Susan Goto (UBC).

2.7.2 Phospho-Peptide Mapping

The bands corresponding to FLAG-TSC1 were excised from the SDS-PAGE gel according to the X-ray film. This has to be done very precisely to prevent contamination from other proteins in the gel and/or loss of the target protein. The excised gel pieces were transferred to a clean glass plate on which they were diced into small cubes (1 mm^3) to facilitate exposure to protease in subsequent reduction and alkylation steps. Gel pieces were then transferred into clean microfuge tube. To reduce the reactive thiol groups (-SH), gel pieces were incubated with 150 μl of 10 mM DTT in 100 mM NH_4HCO_3 at room temperature for 15 min under constant agitation (1100 rpm). After the supernatant was removed, reduced gel pieces were incubated with 150 μl of 50 mM iodoacetamide in 100 mM NH_4HCO_3 and covered with foil at room temperature for 30 min with constant agitation. The gel pieces were washed with 300 μl 100 mM NH_4HCO_3 and further

washed with 300 µl 50% acetonitrile (CH_3CN) in 20 mM NH_4HCO_3 with both washes lasting 15 min and done under room temperature and constant agitation. The sample was then dried in a Vacufuge™ (Eppendorf) for 30 min at 30ºC. The gel pieces were then subjected to *in gel* proteolytic digestion with 12.5 µg/ml of modified trypsin in 20 mM NH_4HCO_3 and 0.1%n-octyl glucoside for 16 h at 30ºC under constant agitation. The digested peptides were extracted from the gel pieces by adding an equal volume of 100% CH_3CN to the digestion mixture and incubating at 30ºC for 30 min. The radioactivity in the band pieces and supernatant was measured by a scintillation counter (Cerenkov Mode). Extraction was repeated with CH_3CN if significant amount of radioactivity still remained with the gel pieces. The supernatant containing the digested FLAG-TSC1 peptide was dried down. Dried peptide was then resuspended in 5 µl of first dimension buffer (2.5% (v/v) formic acid, 7.8% (v/v) acetic acid). The peptides were loaded onto a thin-layer chromatography (TLC) plate (20 cm x 20 cm) 0.5 µl at a time to avoid smearing and were then separated by electrophoresis at 800 V for 90 min in first dimension buffer. Then, TLC plates were placed in secondary dimension buffer (62% (v/v) isobutyric acid, 1.9% (v/v) n-butanol, 4.8% (v/v) pyridine and 2.9% (v/v) acetic acid) to separate the peptides by chromatography. Once the buffer front was approximately 2 cm from the top of the plate, the TLC plate was removed from the buffer and dried. Radiolabelled peptides were then visualized by exposure to a storage phosphor screen (GE Healthcare) and scanned by a Typhoon™ 8600 Phosphorimager (Molecular Dynamics).

Chapter 3

4E-BP1 in protein synthesis and growth in ARVC

3.1 Introduction

It was previously shown that hypertrophic agent PE elicits an acute activation of protein synthesis in ARVC, which is largely blocked by rapamycin, (Wang and Proud, 2002). This indicates a key role for signalling through mTORC1 in activating protein synthesis and provides a physiologically relevant primary cell system for analyzing which component(s) downstream of mTORC1 is/are involved in the activation of protein synthesis. The best-studied targets of mTORC1 are the S6 kinases and the 4E-BPs. Earlier data from S6K1/S6K2 knockout mice revealed that these enzymes were not required for cardiac hypertrophy in response to overload or exercise (McMullen and Shioi et al., 2004). They do not therefore appear to play a role in physiological or pathological cardiac hypertrophy. Accordingly, we next focused our attention on 4E-BP1 and the formation of eIF4E/eIF4G complexes, since it is widely believed that they play a major role in the control of protein synthesis, due to the involvement of eIF4G in interacting with many translational components, and in thereby recruiting the 40S subunit to the mRNA to initiate translation (Gingras and Raught et al., 2001; Pestova and Kolupaeva et al., 2001; Fingar and Blenis, 2004). This therefore provides a mechanism by which signalling through mTORC1 could promote translation initiation.

3.2 Result

3.2.1 Overexpression of 4E-BP1 abolishes eIF4F complex formation

It has been reported in ARVC that PE treatment induces formation of eIF4F (or an increased association of eIF4E and eIF4G) and this event is sensitive to rapamycin (Wang and Proud, 2002). 4E-BP1 shares a similar eIF4E binding motif with eIF4G, hence is able to competitively inhibit eIF4G and eIF4E interaction. Phosphorylation of 4E-BP1 upon mTORC1 activation leads to its dissociation from eIF4E, freeing eIF4E to bind the scaffold protein eIF4G and form the eIF4F initiation complexes which may include other additional components, such as eIF4A. The formation of such complexes, rather than the phosphorylation of 4E-BP1 itself, is the important parameter for the regulation of translation initiation. Therefore, to study the potential regulatory role of 4E-BP1 and eIF4F complex on other parameters such as translation initiation and cell growth, it was necessary to confirm that the amount of ectopically expressed 4E-BP1 was enough to completely prevent any formation of eIF4F in both basal and excited states. Two adenoviruses encoding the wild type 4E-BP1 or a mutant 4E-BP1 which cannot bind to eIF4E were created. In the LM/AA mutant form of 4E-BP1, two mutations were introduced in the eIF4E-binding motif shared by eIF4G to render it inactive in the sense of binding to eIF4E (Figure 3.2.1.B).

To assess the binding of eIF4G to eIF4E, eIF4E, along with any associated proteins, was purified by affinity chromatography on m^7GTP-Sepharose, which mimics the structure of the 7-methyl-guanosine structure of the 5' cap. As shown in Figure 3.2.1A, in

cells expressing GFP and the LM/AA mutant 4E-BP1, limited amount of eIF4G was associated with eIF4E in the ground state. There was also a substantial amount of 4E-BP1 bound to eIF4E. Upon treatment with PE, 4E-BP1 binding was reduced, thereby greatly enhancing eIF4G binding as reported earlier (Wang and Proud, 2002). On the other hand, the ectopically expressed wild type 4E-BP1 remained bound to eIF4E regardless of PE stimulation, blocking basal and PE-induced eIF4G binding. This is indeed what was expected: the functional disruption of translation initiation by preventing the formation of eIF4F complexes (eIF4G binding to eIF4E). It is likely that the excessive amount of 4E-BP1 overloads the cellular capacity of mTOR signalling or other potential means to phosphorylate all 4E-BP1 so that enough 4E-BP1 molecules remain hypophosphorylated and retain eIF4E binding ability, thereby excluding eIF4G.

The above results established a firm foundation for me to assess the role of eIF4F assembly in the regulation of protein synthesis and cell growth. However, it was crucial to establish that the high levels of 4E-BP1 that was achieved by adenovirus gene transfer did not interfere with other signalling events downstream of mTORC1. Because p70 S6K1 and 4E-BP1, among the many mTORC1 targets, are recognized by the raptor component of mTORC1 through their TOS motifs (Schalm and Fingar et al., 2003), it was possible that the high levels of ectopically expressed 4E-BP1 may overwhelm the mTORC1 kinase machinery by sequestering it through binding with raptor leading to unintended impairment of signalling to other mTORC1 targets.

To study this, ARVC were infected with adenoviruses encoding GFP, wild type

4E-BP1, or the LM/AA form of 4E-BP1 as a negative control, and were stimulated with PE as indicated. The phosphorylation states of three well-established mTORC1 targets were analyzed by SDS-PAGE and western blotting. First, the phosphorylation status of 4E-BP1 was revealed by the migration rate through SDS-PAGE or detected by phosphor-specific antibodies in western blot. 4E-BP1 can be resolved into multiple species (α, β, and γ) on SDS-PAGE (using gels containing 13.5% acrylamide and 0.36% bisacrylamide) according to the degree of phosphorylation with the hyperphosphorylated γ form being the slowest and the hypophosphorylated α form running the fastest. As shown in Figure 3.2.1.C, in the unstimulated state, most 4E-BP1 exists in the faster running β form (less phosphorylated) and the α form (hypophosphorylated). As reported earlier by preceding lab members (Wang and Proud, 2002), PE induced the phosphorylation of 4E-BP1 and led to an increase in the γ form (hyperphosphorylated) of the 4E-BP1 population on SDS-PAGE. The above result was again confirmed by immunoblotting with a phosphor-specific antibody that reacts with 4E-BP1 only when it is phosphorylated at Ser64. In the unstimulated state, there was barely any signal whereas in PE-stimulated samples the Ser64 phosphorylation of 4E-BP1 became evident.

A second well-known target of mTORC1 signalling are the ribosomal protein S6 kinases, S6K1 and S6K2, both of which are directly phosphorylated by mTORC1 and expressed in ARVC (Wang and Wang et al., 2000; Wang and Gout et al., 2001). The kinase activity of S6Ks can be easily assessed by monitoring the phosphorylation of their substrate, ribosomal protein S6, by phosphor-specific antibodies. Upon PE stimulation,

S6 kinases were readily activated and phosphorylation on Ser235/6 of S6 became apparent.

Thirdly, eEF2 is also a primary target under the regulation of mTORC1 through eEF2 kinase, which is the only mammalian kinase known to phosphorylate eEF2 (Browne and Proud, 2002). Under basal conditions, eEF2 is phosphorylated at Thr56, which is regulated in an mTORC1-dependent manner (Browne and Proud, 2002). The exact mechanism of how mTORC1 regulates eEF2 kinase and eEF2 phosphorylation remains unclear. Yet, upon mTORC1 signalling activation, eEF2 becomes dephosphorylated and active (Wang and Proud, 2002). In Figure 3.2.1.C, eEF2 was mostly phosphorylated at basal state and became majorly dephosphorylated upon PE treatment regardless of which adenovirus had been used.

It is evident from these data that PE induced very similar changes in the phosphorylation of endogenous 4E-BP1, S6 or eEF2 in ARVC irrespective of whether they expressed WT or mutant 4E-BP1, or GFP. Thus, it is clear that expressing ectopic 4E-BP1 at high levels does not interfere with mTORC1 signalling. This system can, therefore, be used to study the importance of eIF4F complex for the control of protein synthesis by mTORC1 signalling.

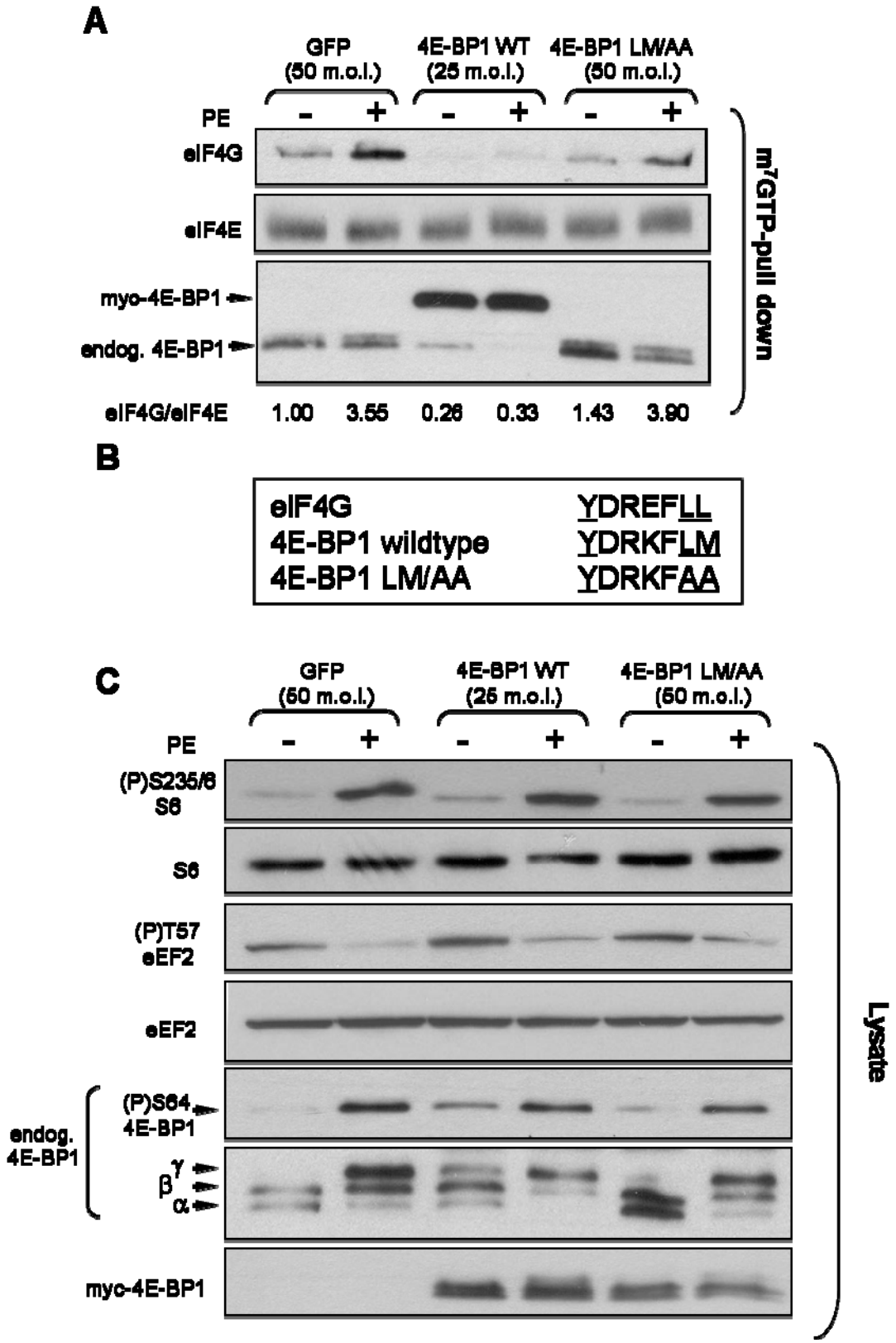
A
GFP
(50 m.o.l.)
4E-BP1 WT
(25 m.o.l.)
4E-BP1 LM/AA
(50 m.o.l.)
PE
- + - + - +
eIF4G
eIF4E
myo-4E-BP1
endog. 4E-BP1
m7GTP-pull down
eIF4G/eIF4E 1.00 3.55 0.26 0.33 1.43 3.90
B
eIF4G YDREFLL
4E-BP1 wildtype YDRKFLM
4E-BP1 LM/AA YDRKFAA
C
GFP
(50 m.o.l.)
4E-BP1 WT
(25 m.o.l.)
4E-BP1 LM/AA
(50 m.o.l.)
PE
- + - + - +
(P)S235/6 S6
S6
(P)T57 eEF2
eEF2
endog. 4E-BP1
(P)S64 4E-BP1
β γ
α
myc-4E-BP1
Lysate

FIGURE 3.2.1. 4E-BP1 blocks eIF4G/eIF4E binding in ARVC. (A) ARVC were infected with adenoviruses encoding GFP (negative control protein), myc-tagged wild type (WT) 4E-BP1 or a mutant of 4E-BP1 in which the eIF4E-binding motif has been mutated so that it cannot bind eIF4E (LM/AA mutation: see panel (B)). Forty h later, some plates were treated with PE (10 μM, 60 min) as indicated. Cytosolic lysates were prepared, and then subjected to affinity chromatography on m^7GTP-Sepharose. The bound material was analysed by SDS-PAGE and immunoblotting using the indicated antibodies. In the bottom section, the positions of the endogenous (endog.) and the ectopically-expressed 4E-BP1 polypeptides are shown. (B) The eIF4E-binding motifs of 4E-BP1 and eIF4G are shown, together with the modified sequence in the LM/AA mutant used here. Residues conserved, or very similar, in different binding partners for eIF4E are underlined. (C) As panel (A) but lysates of ARVC were analysed directly by SDS-PAGE/immunoblot using the indicated antisera. The α, β and γ species of 4E-BP1 are shown (α being the least phosphorylated and γ the most). Data are presented as mean values ± s.e.m. from three independent experiments.

3.2.2 Activation of protein synthesis by PE does not require the increased formation of eIF4E/eIF4G complexes.

In the preceding section, it was firmly established that overexpressing 4E-BP1 blocks the assembly of eIF4F initiation complex, one potential route through which mTOR signalling activates protein synthesis. According to previous reports, PE activates protein synthesis in ARVC by activating mTORC1 (Wang and Proud, 2002). Hence, to assess the importance of the induction of eIF4E/eIF4G binding for the activation of protein synthesis by PE, the rate of incorporation of label (L-[^{35}S]methionine) into protein was measured in cells overexpressing GFP or wild type 4E-BP1 with or without PE stimulation.

As shown in Figure 3.2.2A, PE robustly activated protein synthesis by about 1.8 fold in the GFP control cells. The activation by PE was partially sensitive to rapamycin as previously reported (Wang and Proud, 2002), where the authors described a relatively-small but significant rapamycin-resistant portion of protein synthesis activation induced by PE. Interestingly, in 4E-BP1-expressing cells, the basal rate of protein synthesis was dramatically reduced by 40% when compared with the GFP counterpart. This effect more likely reflects the reduction of the basal levels of eIF4F complexes (Figure 3.2.1), since overexpression of the 4E-BP1 LM/AA mutant, which has no effect on eIF4F assembly, did not cause such a reduction in basal rates of protein synthesis. If the reduction in basal protein synthesis were caused by secondary effects of overexpressing 4E-BP1 but not the loss of eIF4F complexes, the same reduction should

be seen in the 4E-BP1 LM/AA samples since it was overexpressed to similar levels as the wild type protein. This conclusion is consistent with the notion that a greatly reduced pool of available eIF4F would decrease translation initiation and general protein synthesis. This mechanism may account for rapamycin's inhibitory effect basal protein synthesis.

Surprisingly, disruption of the eIF4F complex by overexpressing 4E-BP1 did not lead to any inhibition of the ability of PE to activate protein synthesis. When the reduced basal rate of protein synthesis is taken into account, PE activated protein synthesis to at least the same extent in the cells expressing 4E-BP1 as the GFP control set. In fact, the percentage increase in protein synthesis induced by PE was actually greater in the 4E-BP1-expressing cells (increase of 80% in control cells; 106% in cells expressing 4E-BP1). One may argue that PE might have utilized an mTORC1-independent pathway to activate protein synthesis, therefore making overexpression of 4E-BP1 ineffective to inhibit the upregulation of protein synthesis. To test this possibility we assessed the effect of rapamycin. Rapamycin almost completely blocked PE's stimulatory effect with the presence of ectopically expressed 4E-BP1, indicating that the activation of protein synthesis is still mediated through mTORC1 signalling.

Several important conclusions can be drawn from the above findings: (i) eIF4F complexes are important for maintaining the basal level of mRNA translation in ARVC, (ii) cap-dependent initiation, or the assembly of eIF4F, is not an essential factor for the acute activation of mRNA translation by PE, and (iii) PE activates protein synthesis

through a mechanism that does not require the phosphorylation and inhibition of 4E-BP1, but still involves mTORC1 signalling.

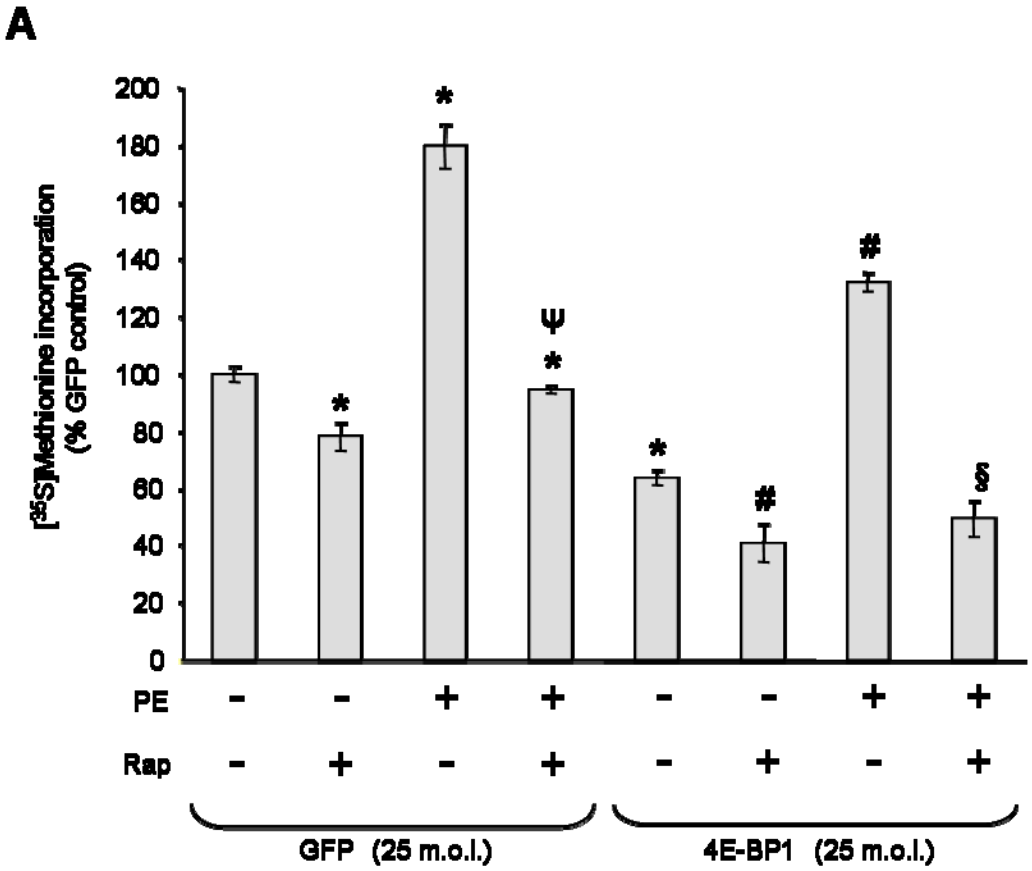

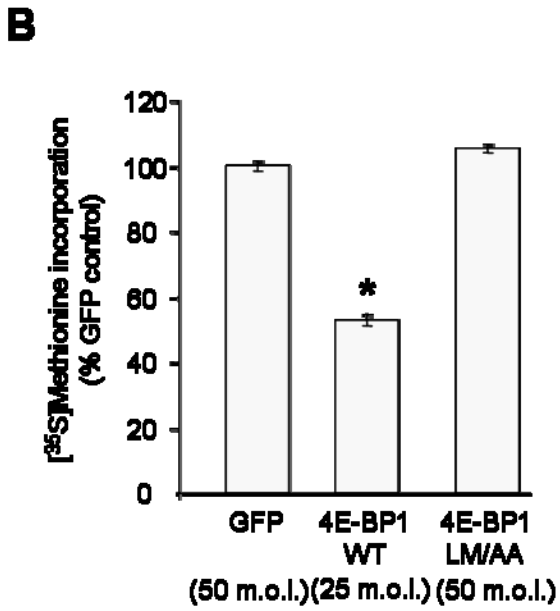

FIGURE 3.2.2. 4E-BP1 does not block the ability of PE to activate protein synthesis in ARVC. (A-B) ARVC were infected with adenoviruses encoding GFP (negative control protein) or myc-tagged 4E-BP1. Forty h later, some plates were treated with PE (10 μM, 90 min) and or treated with rapamycin (100 nM, added 30 min before PE stimulation). 5 μCi/ml L-[^{35}S]methionine was then

added to the medium and 45 min later cells were washed with ice-cold PBS and lysed. Data are corrected for the protein content of the lysate and are normalized to the level of protein synthesis in untreated cells expressing GFP. Data are presented as mean values ± s.e.m. from three independent experiments. The symbols indicate $p < 0.05$ vs. the following controls: * vs. GFP control; # vs. 4E-BP1 control; ψ vs. GFP cells treated with PE; § vs. 4E-BP1-overexpressing cells treated with PE.

Contrary to the general belief that eIF4E/4F is a critical focus for the regulation of translation, these results suggest that the activation of general protein synthesis by hypertrophic agent PE does not involve the upregulation of general translation initiation mediated by eIF4F. To make certain that the radioactivity detected by the scintillation counter actually reflects the incorporation of radioactive labels into newly synthesized proteins via mRNA translation but not through other means, a translation elongation inhibitor cycloheximide (CHX) was introduced to ARVC prior to the addition of [^{35}S]methionine. The results (Figure 3.2.3) analyzed by SDS-PAGE and autoradiograph showed that CHX treatment almost brought a complete halt of protein synthesis and eliminated almost all the labelling. This confirms that the incorporation of radiolabelled amino acid was indeed due to protein synthesis.

The autoradiograph (Figure 3.2.3) also confirmed the conclusions from the previous section that PE can activate protein synthesis independent of translation initiation mediated by eIF4F. Upon PE stimulation, the general incorporation of radioactive methionine into proteins still rose significantly despite the absence of eIF4F. The activation of protein synthesis was strongly inhibited by rapamycin. There was no apparent difference in regulation of any specific sets of proteins, thereby confirming that mTORC1 signalling regulates the translation of the majority of the mRNA population without involving eIF4F and 4E-BP1. However, 4E-BP1 could still regulate certain subsets of mRNA whose low abundance products were not observed using this method.

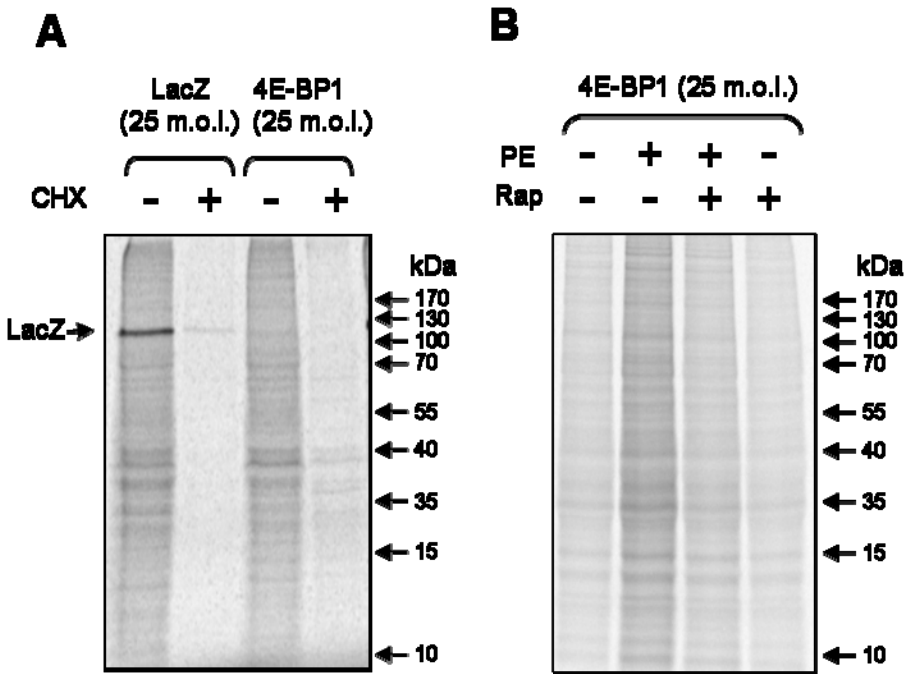

FIGURE 3.2.3. Effects of 4E-BP1 and cycloheximide (CHX) on protein synthesis in ARVC. (A) ARVC were infected with viruses encoding lacZ or 4E-BP1 as indicated. After transfer to methionine-free medium for 2 h, cells were treated with CHX (20 μg/ml, 90 min) and then labelled with 20 μCi/ml L-[^{35}S]methionine for another 6 h. Cells were lysed and labelled proteins were analysed by SDS-PAGE followed by visualization using a phosphorimager. The positions of molecular weight markers and of lacZ are indicated by arrows. Data presented are representative figures of three independent experiments. (B) ARVC were infected with the virus encoding 4E-BP1. After transfer to methionine-free medium for 2 h, cells were treated with PE (10 μM, 90 min) and/or rapamycin (100 nM, 30 min before PE treatment) and then labelled with 20 μCi/ml L-[^{35}S]methionine. Cells were lysed and analysed as in (A). Data presented are representative figures of three independent experiments.

3.2.3 4E-BP1 does not block PE-induced heart cell growth

Enhanced protein synthesis is one of the main driving forces for hypertrophy of cardiomyocytes (Hannan and Jenkins et al., 2003). Although 4E-BP1 was shown to play an insignificant role in the acute activation of protein synthesis by PE in last section, it might have an effect in the long run especially considering it has a profound inhibitory effect on the basal rate of protein synthesis. Theoretically, to increase translational output, the cells may increase translation efficiency for a short term response or they may opt to augment translation capacity (i.e. the number of ribosomes) to sustain a long term need, for example cell hypertrophy. Therefore, it was important to investigate whether 4E-BP1 influenced the development of cardiomyocyte hypertrophy (cell growth).

Measuring cross-sectional cell area is a common method for estimating cardiomyocyte size (Purcell and Tang et al., 2001; Wullschleger and Loewith et al., 2006). Wang et al. also showed that cross-sectional area is an accurate estimation of the cardiomyocyte volume and therefore the actual three-dimensional cell size (Wang et al., 2008 submitted). By this approach, it was shown that PE increased the cross-sectional area of ARVC dramatically in the control group, and this increase was entirely inhibited by rapamycin confirming that mTORC1 signalling plays an essential and central role in the development of hypertrophy. In the experimental group which was infected with the 4E-BP1 adenovirus, the lower basal rate of protein synthesis (Figure 3.2.4) did not result in a smaller cell size. The loss of eIF4F was reflected in a small but statistically significant ($p < 0.05$) reduction in cell size during PE stimulation which still brought

about a substantial increase in cell hypertrophy in the presence of 4E-BP1. Although the percentage increase of protein synthesis induced by PE was not diminished by overexpression of 4E-BP1, the reduction in the absolute value of protein synthesis may have limited the ability of cardiomyocytes to grow (Figure 3.2.2 and Figure 3.2.4). Nonetheless, rapamycin, consistent with previous findings, entirely negated the remaining cell growth indicating that PE treatment depends on mTORC1 signalling to induce cardiomyocyte hypertrophy.

Combining the findings from this section and the previous sections, it is concluded that the hypertrophic response to PE and its required upregulation of protein synthesis operate independently of the formation of eIF4F complexes.

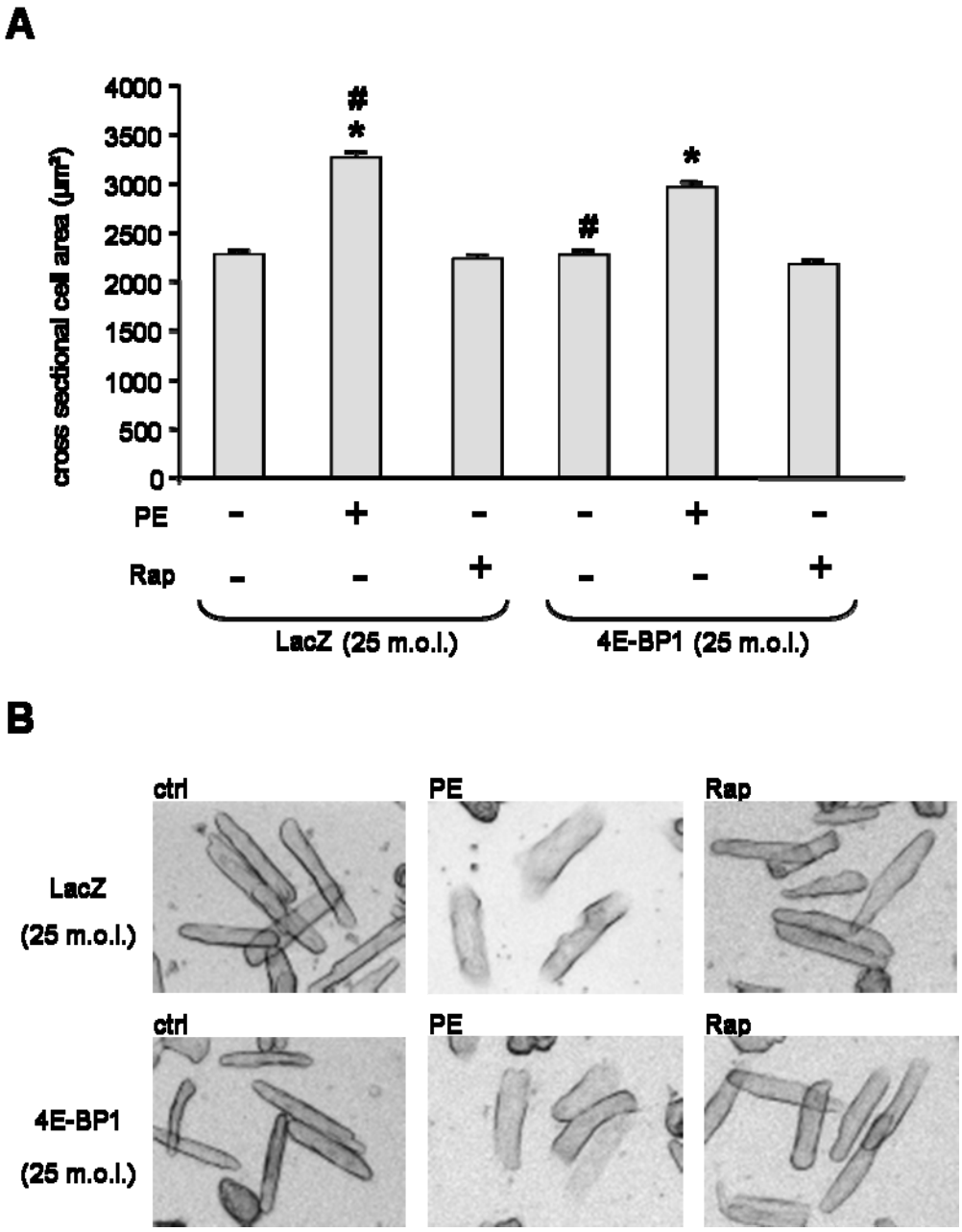

FIGURE 3.2.4. 4E-BP1 does not block PE-promoted ARVC growth. (A-B) ARVC were infected with adenoviruses encoding lacZ (negative control protein) or myc-tagged 4E-BP1. After removing the adenoviruses, some plates were treated with PE (10 μM, 40 h) and, in some cases, also with rapamycin (100 nM, added 30 min before PE stimulation). Cell area was determined for at least 80 cells in each condition. Data (mean values ± s.e.m.) presented is a representative figure of three independent experiments. * Indicates $p < 0.05$ vs. lacZ control; # $p < 0.05$ vs. 4E-BP1-overexpressing cells treated with PE.

3.2.4 4E-BP1 suppresses the PE-induced activation of the translation of 'structured' mRNAs

It is possible that the PE stimulated the majority of the entire mRNA population that to increase translation efficiency independent of eIF4F while the effects of 4E-BP1 on specific subsets were overlooked. For example, it has been reported that eIF4F is required to facilitate translation of mRNAs with highly structured 5'-UTRs (untranslated regions) (Pestova and Kolupaeva et al., 2001). Structured 5'UTRs could potentially prevent the access of ribosomes to the start codon on the mRNA by interfering with scanning. eIF4A, a component of eIF4F complex, is an RNA helicase that can unwind secondary structure in the 5'UTR and thereby allow translation initiation (Pestova and Kolupaeva et al., 2001). Therefore, it was of particular interest to examine whether overexpression of 4E-BP1 influenced the translation of mRNAs with different degrees of structured 5'UTRs. The McDermott laboratory created a set of adenoviral luciferase reporters that encode a reporter gene, luciferase, downstream of varying structured 5'UTRs (Figure 3.2.5A) (Tuxworth and Saghir et al., 2004). The "B0" adenovirus is moderately structured in its 5'UTR with a predicted Gibbs free melting energy of -57 kcal/mol whereas the "B4" adenovirus contains a more heavily structured 5'UTR (four contiguous BamH1 inserts) with a predicted Gibbs free melting energy of -122 kcal/mol. Figure 3.2.5.A shows a schematic representation of the two different constructs.

To ensure that sufficient 4E-BP1 was present before the luciferase mRNA started to be translated, ARVC were first infected with control lacZ and wild type 4E-BP1

adenoviruses, and 16 h later the cells were infected with the adenoviral luciferase reporters and stimulated with PE as indicated. The cells were allowed to express and accumulate luciferase for 20 h before they were lysed and luciferase assays (Promega kit) were performed to estimate how much luciferase had been made. All assays were performed within the linear range and the results were normalized for the amount of luciferase mRNA as determined by qRT-PCR in each experimental condition tested.

Under basal conditions where PE was not administered, the "B4" luciferase construct was expressed at a lower level, as expected, than the "B0" luciferase construct when the level of both mRNA levels were taken into account (Figure 3.2.5.B). PE treatment stimulated the expression from both vectors very markedly. The "B0" construct showed an increase in expression of 1424±46% from the unstimulated control condition whereas the increase for "B4" construct was 1172±67%. The increase in the reporter's expression in both constructs upon PE stimulation is quite similar. This indicates that PE was able to overcome the translation suppression from the highly structured 5'UTR of the "B4" construct presumably by inhibiting 4E-BP1 and promoting eIF4F assembly, and thus leads to an efficient translation of the construct. This finding is consistent with the proposed function of eIF4F, which is to facilitate ribosome start codon scanning through the melting of secondary mRNA structures in the 5' UTR. The activation of translation of these structured mRNA is much higher than that of general protein synthesis estimated by radiolabel incorporation (Figure 3.2.2). This could be explained by the fact that the secondary structures in the 5'UTRs of these mRNAs limit their translation efficiency

under unstimulated conditions whereas general mRNAs in the cell undergo translation with much less hindrance (less secondary structure).

The presence of ectopically expressed 4E-BP1 severely limited the ability of PE to upregulate the translation of the "B0" construct while completely preventing any translation activation for the "B4" construct (Figure 3.2.5.B). This finding strongly suggests that although the activation of general protein synthesis is independent of the induction of eIF4F formation upon PE stimulation, eIF4F is critical for the upregulation of specific subsets of mRNAs, especially those with highly structured 5'UTRs.

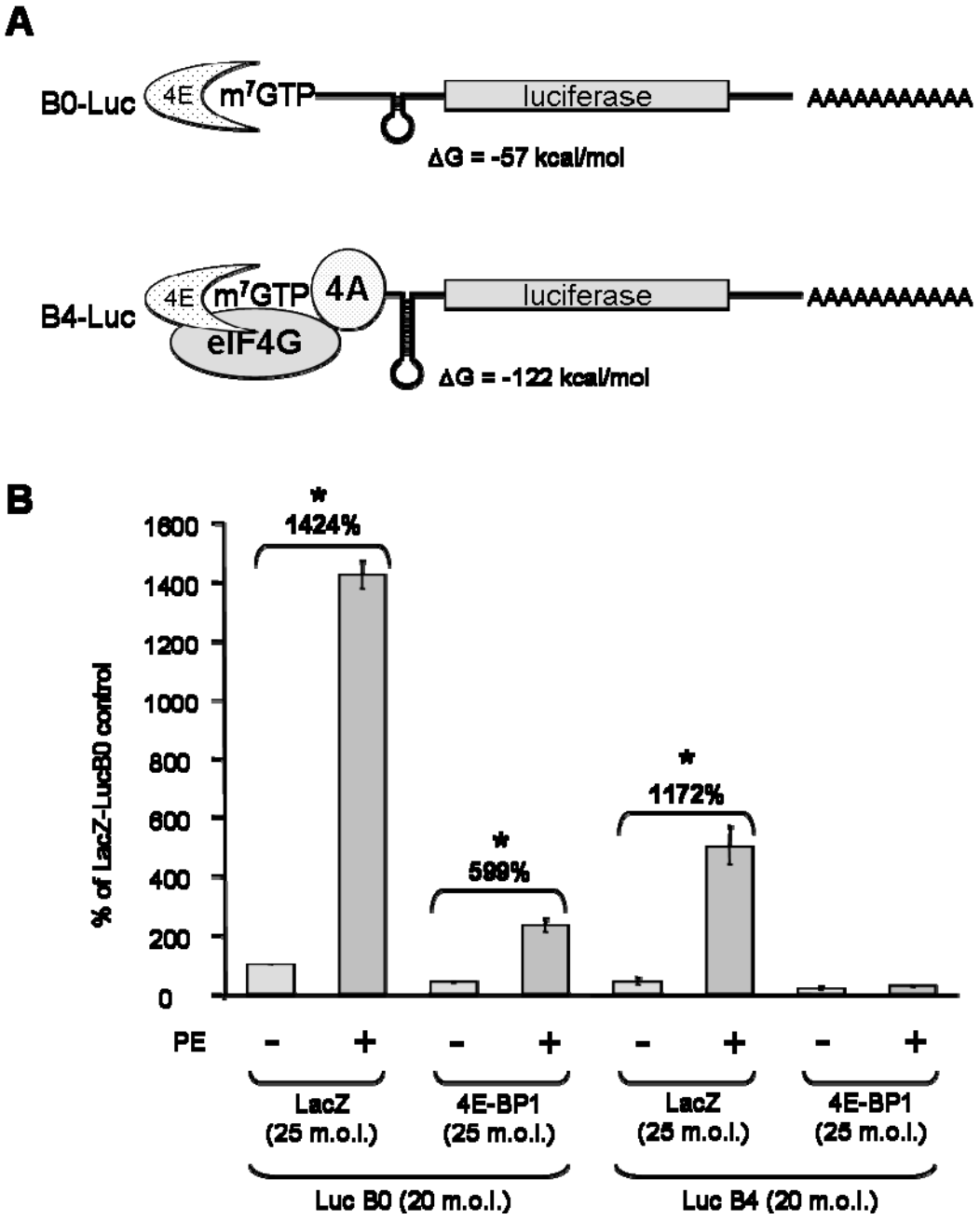

FIGURE 3.2.5. Analysis of the effects of expressing 4E-BP1 on luciferase reporters. (A) Schematic illustration of the 'B0' and 'B4' vectors used in this study: both adenoviral vectors encode luciferase, but B4 contains more extensive secondary structure in its 5'-UTR and its translation is therefore predicted to more heavily dependent upon eIF4F complexes, specifically the eIF4A (RNA helicase) component. (B) ARVC were infected with adenoviruses encoding lacZ or WT 4E-BP1 after cell isolation and with either the B0 or B4 luciferase virus 16 h later. Then, cells were treated with 10 μM PE for 20 h. Lysates were processed for measurement of luciferase activity and RNA extraction for qRT-PCR. Data are corrected for the relative levels of the reporter mRNAs and are normalized to the lacZ B0 control. Data are presented as mean values ± s.e.m. from three independent experiments.

3.3 Discussion

This section of the study focused on investigating the role of eIF4F in the regulation of protein synthesis. To eliminate eIF4F complex formation even under growth stimulating conditions (PE treatment), enough ectopic 4E-BP1 was overexpressed to the extent that almost all the eIF4E was sequestered as eIF4E-4E-BP1 complexes. Through this approach, three important conclusions were drawn. First, it was discovered that the complete loss of eIF4F complexes resulted in a reduced basal protein synthesis rate. One may wonder how protein synthesis could be sustained if *de novo* translation initiation was impossible. My result is indeed consistent with the idea that mRNA already engaged in ongoing translation can reload ribosomes for subsequent rounds of translation (undergo 're-initiation') independently of functional eIF4F complexes. Previous findings showed that proteolytic cleavage of eIF4G, which renders it inactive, does not prevent ongoing mRNA translation (Novoa and Carrasco, 1999). It is possible that through the circularization of mRNAs that are being translated, dissociated ribosomal subunits become so locally concentrated near the 5'UTRs of the mRNA that they do not require active eIF4F complexes to interact with the mRNAs anymore. It is likely that the remaining basal protein synthesis reflects the portion of mRNAs that are constantly being translated and have ribosomes already on them, thus making them insensitive to the loss of eIF4F. Secondly, it was demonstrated that the mTORC1-dependent activation of protein synthesis is entirely independent of eIF4F complexes. It is a rather surprising finding as eIF4F is generally regarded as the main regulator of translation initiation. My

data clearly show that even in the virtual absence of eIF4F complex, phenylephrine activates protein synthesis to the same degree as in control ARVC. This finding complements earlier findings that suggest translation efficiency can be increased without functional eIF4F (Novoa and Carrasco, 1999). Thirdly, it was demonstrated that the stimulation of protein synthesis in ARVC overexpressing 4E-BP1 remains highly sensitive to inhibition by rapamycin. In conclusion, my results suggest that phenylephrine induced activation of protein synthesis in ARVC is dependent on mTORC1 signalling and likely involves other downstream targets, but not 4E-BP1.

We are not the first group to suggest that eIF4F does not play a crucial role in the regulation of protein synthesis, although those studies used a different approach and did not study the role of mTORC1. Previous results show that overexpression of the cap-binding protein, eIF4E, induced increased levels of eIF4F assembly but could not bring an enhancement of the overall rate of protein synthesis in adult feline cardiomyocytes (Saghir and Tuxworth et al., 2001). Similarly, eIF4F level in cardiomyocyte was also shown to have no effect on the translation efficiency of the B0 and B4 luciferase reporters [Saghir, 2001; Tuxworth, 2004]. This finding agrees well with other cell types as similar findings have been recently reported in human embryonic kidney 293 cells (Wang and Proud, 2008).

Other labs have also attempted to investigate the functional significance of eIF4F by generating transgenic mice by knocking out 4E-BP1 alone or with 4E-BP2. These are the two major 4E-BP isoforms expressed in cardiomyocytes. The 4E-BP1 single knockout

and 4E-BP1/2 double knockout mice did not show any changes in the mass of their hearts (Tsukiyama-Kohara and Poulin et al., 2001; Le and Petroulakis et al., 2007). These results imply that 4E-BP1/2 and eIF4F are unlikely to be key components for the regulation of cardiomyocyte size. My result may provide an explanation for this observation by showing that increased levels of eIF4F upon acute PE stimulation are not essential for induction of protein synthesis, which is one of the requirements for sustained cell growth. In addition, it was found that in the complete absence of eIF4F, there was no effect to PE's ability to activate protein synthesis. These findings are rather unexpected. It is generally believed that the formation of eIF4F complexes important for the regulation of protein synthesis by controlling the early steps in translation initiation. It may be that PE actually stimulates translation of mRNAs that no longer need eIF4F to recruit ribosome, for example, the pre-engaged mRNAs. Pre-engaged mRNAs are mRNAs that are already associated with polysomes. In fact, it has been shown before that functional eIF4F complex is not required for ongoing translation, although that study did not explain the regulation of translation of the role of mTORC1 signalling (Novoa and Carrasco, 1999). Consistent with the above, overexpression of wild type 4E-BP1 decreased, but did not eliminate, basal rates of protein synthesis. In this case, loss of eIF4F may cause the inability of the cell to promote the interaction of newly synthesized mRNAs with ribosomes leading to a reduction in basal protein synthesis while pre-engaged mRNAs continue to be translated.

Even though these results suggest that eIF4F complexes are not involved in the

upregulation of general protein synthesis, it is entirely possible that they may regulate the translation efficiency of certain sub-groups of the mRNA population, such as mRNAs with highly structured 5'UTRs. Indeed, by utilizing reporter constructs that contain different degrees of secondary structure, we showed that overexpressing 4E-BP1 completely eliminated the ability of PE to increase the expression of the reporter from the highly structured mRNA (Luciferase B4). Although the mTORC1-dependent formation of eIF4F complexes (and thus the control of eIF4E and 4E-BP1) does not play a major role in the rapamycin-sensitive activation of protein synthesis, the above data clearly showed that eIF4F complexes could be important for the efficient translation of certain specific mRNAs. Since no changes were observed on SDS-PAGE analysis, such mRNAs most likely encode low-abundance proteins.

Although we were unable to pinpoint the mTORC1-regulated translation component that is responsible for the mTORC1-dependent stimulation of general mRNA translation, these data combined with previous findings (McMullen and Shioi et al., 2004) show that 4E-BP1 and S6 kinases are most likely not major contributors. It remains important to characterize the functional significance of the PE-induced mTORC1-dependent dephosphorylation and activation of eEF2 (required for translation elongation of all mRNAs) in the context of protein synthesis and cell growth.

Chapter 4

The classical MEK/Erk pathway regulates the TSC1/2 complex

4.1 Introduction

Since mTORC1 signalling plays a central role in the regulation of protein synthesis, it is essential to understand how the activation of the classical MEK/Erk pathway brings about the inactivation of TSC1/2 complex and the subsequent activation of mTORC1 signalling. Previous reports (Rolfe and McLeod et al., 2005) have shown that TSC2 undergoes regulated phosphorylation in HEK293 cells in response to PMA treatment through the MEK/Erk pathway (discussed in section 1.8) at sites that cross-react with a commercially available "anti-phospho Akt-substrate" antibody. This antibody detects phosphorylation of serine and threonine residues that are preceded by arginines at position -3 and -5 (RXRXXS/T); it is the consensus target sequence for Akt (PKB), but also for other AGC (protein kinase A/protein kinase G/protein kinase C) kinases such as the $p90^{RSKs}$. It was empirically determined that the "anti-phospho Akt-substrate" antibody detects phosphorylation at Ser1798 (RKRLIS) in response to PMA as shown by the observation that mutating Ser1798 to alanine abolished the reactivity with this antibody (Rolfe and McLeod et al., 2005). Phosphorylation at this site is unlikely to be mediated by Akt because the activation of MEK/Erk pathway does not activate Akt (Wang and Gout et al., 2001). It was unclear how MEK/Erk signalling leads to TSC2 phosphorylation in response to PMA and PE (Roux and Ballif et al., 2004; Ballif and Roux et al., 2005; Rolfe and McLeod et al., 2005). Previous literature supported the hypothesis that $p90^{RSKs}$, which is immediately downstream of Erk, mediates the phosphorylation of TSC2 and leads to activation of mTORC1 after PMA stimulation

(Roux and Ballif et al., 2004; Ballif and Roux et al., 2005). On the other hand, it has also been reported that Erk directly phosphorylates TSC2 (Ma and Chen et al., 2005). A recently available $p90^{RSKs}$-specific inhibitor BI-D1870 (Sapkota and Cummings et al., 2007) allows us to dissect this system.

4.2 Results

4.2.1 BI-D1870 does not inhibit PE-induced mTORC1 activation in cardiomyocytes

Most studies use PMA, a potent but non-physiological activator of several members of the PKC family, to stimulate the MEK/Erk pathway and upregulate mTORC1 signalling in cell lines such as HEK293. I wished to re-evaluate the role of the MEK/Erk pathway in the control of mTORC1 signalling by phenylephrine (PE) in cardiomyocytes. PE is an α_1-adrenergic agonist that acts via physiologically relevant receptors to activate PKCδ/ε (Wang and Rolfe et al., 2003) and, in primary cardiomyocytes, it also triggers hypertrophic responses including fetal gene expression and enhanced protein synthesis (Barron and Finn et al., 2003). PE treatment in ARVC causes the phosphorylation and activation of Erk and this is needed for protein synthesis activation (Wang and Proud, 2002). Therefore, it is of particular interest for my study to understand how the MEK/Erk module regulates mTORC1 signalling in response to this hypertrophic agent.

Two mTORC1 signalling targets, 4E-BP1 and ribosomal protein S6, become phosphorylated upon stimulation of ARVC with PE. Most of 4E-BP1 shifted from the faster-moving hypophosphorylated α and β forms to the slower-migrating hyperphosphorylated γ form while phosphorylation of S6 increased as determined by probing the western blot with the anti-phospho-Ser235/6 antibody (Figure 4.2.1A). The ability of rapamycin and PD098059 (MEK inhibitor) to abolish these phosphorylation events confirmed previous data that PE activates mTORC1 signalling via the MEK/Erk

pathway to phosphorylate mTORC1 targets. The observation that phosphorylation of S6 was completely inhibited by rapamycin indicates that the phosphorylation is a direct action of the S6Ks downstream of mTORC1 and not a consequence of S6 phosphorylation by $p90^{RSKs}$, which phosphorylates S6 directly in other cell types (Fonseca, 2008 unpublished). PE activates both isoforms of S6Ks in ARVC (Wang and Gout et al., 2001; Wang and Proud, 2002).

Rapid and sustained activation of $p90^{RSKs}$ is induced by PE in ARVC (Wang and Proud, 2002). PE also leads to the phosphorylation of TSC2 on Ser1798 (Rolfe and McLeod et al., 2005), which can be readily detected by the "anti-phospho Akt-substrate" antibody. While the low level of endogenous TSC2 makes the detection of its phosphorylation challenging, it is still evident that PE-induced TSC2 phosphorylation was susceptible to treatment of $p90^{RSKs}$ inhibitor BI-D1870 even at a low dosage of 5 μM (Figure 4.2.1B). At higher concentrations of BI-D1870 (10 and 20 μM), anti-phospho Akt-substrate antibody could not detect any residual phosphorylation. In addition, BI-D1870 increased the phosphorylation of Erk1/2 at all concentrations, as reported by Sapkota et al. (Sapkota and Cummings et al., 2007). My results further strengthen the idea that there exists a negative feedback loop from $p90^{RSKs}$ to regulate its upstream activator Erk1/2. All in all, these data demonstrated that BI-D1870 unambiguously repressed $p90^{RSKs}$ activity in ARVC and showed that phosphorylation of Ser1798 in TSC2 depends on $p90^{RSKs}$.

The confirmation that BI-D1870 effectively inhibited $p90^{RSKs}$ activity in ARVC

provides a firm foundation to investigate whether phosphorylation of TSC2 by $p90^{RSKs}$ was important for the activation of mTORC1 signalling by PE. While rapamycin completely inhibited the phosphorylation of Ser64 in 4E-BP1 and of Ser235/236/240/244 in S6 (Figure 4.2.1A) when ARVC were stimulated with PE, BI-D1870 had absolutely no inhibitory effect on these events at any concentration used (up to 20 μM; Figure 4.2.1C). Since PE-induced phosphorylation of Ser235/236/240/244 in S6 is entirely dependent upon signalling through mTORC1 (Figure 4.2.1C) and was not diminished by inhibiting $p90^{RSKs}$, $p90^{RSKs}$ is most unlikely to contribute directly to S6 phosphorylation in ARVC. In fact, it was discovered that BI-D1870 actually enhanced the phosphorylation of 4E-BP1 and of S6 at the aforementioned sites. This phenomenon could be a result of BI-D1870 relieving the inhibitory activity of $p90^{RSKs}$ on Erk, thus enhancing Erk activity and causing a greater activation of mTORC1. The observation that mTORC1 signalling showed an upward trend with increasing dosage of BI-D1870 further reinforced the operation of a feedback loop from $p90^{RSKs}$ to regulate Erk activity. These results strongly imply that neither $p90^{RSKs}$ activity nor $p90^{RSKs}$-regulated TSC2 Ser1798 phosphorylation is required for the activation of mTORC1 signalling by the α_1-adrenergic agonist PE, which activates mTORC1 by a MEK-dependent pathway (Wang and Proud, 2002).

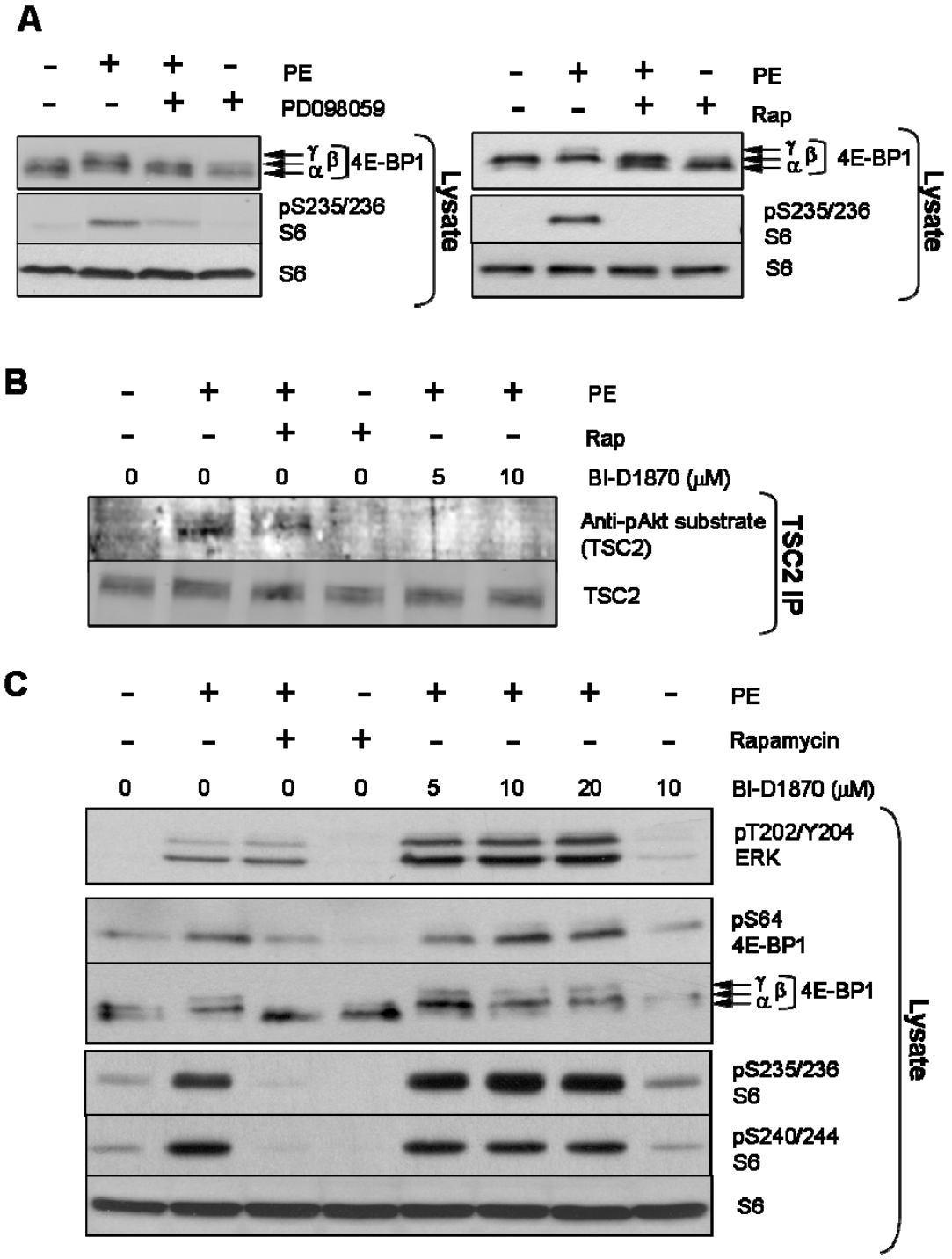

FIGURE 4.2.1. The p90^{RSKs} inhibitor, BI-D1870, does not impair the phenylephrine (PE)-induced activation of mTORC1 signalling in adult rat ventricular cardiomyocytes (ARVC). (A-C) ARVC were treated with 50 μM PD098059 (30 min), 100 nM rapamycin (30 min) or varying concentrations of BI-D1870 (60 min), prior to stimulation with 10 μM PE (60 min) as indicated. In (A,C), samples of lysate (containing equal amounts of protein, typically 30 to 40 μg) were analyzed by SDS-PAGE and western blot, using the indicated antisera. In (B), 1 mg of cell lysate was subjected to

immunoprecipitation using anti-TSC2 antibody. Immunoprecipitates were probed with anti-phospho Akt-substrate or anti-TSC2 antisera as indicated.

4.2.2 TSC1 undergoes regulated phosphorylation *in vivo* and *in vitro*

Although TSC1 has not received much attention compared to its partner TSC2 in the regulation of mTORC1 signalling, TSC1 has also been speculated to undergo regulated phosphorylation (Lee and Kuo et al., 2007; Wu and Zhou, 2007). To confirm these observations, FLAG-TSC1 was overexpressed in HEK293 cells, which had been radiolabelled with ^{32}P. After immunoprecipitation, TSC1 underwent tryptic digestion and the resultant peptides were analyzed by two dimensional peptide map analysis. These experiments were done with HEK293 cells instead of cardiomyocytes because cell lines are more easily manipulated genetically whereas it would involve constructing adenoviruses in ARVC.

In the control sample, TSC1 appeared to be phosphorylated basally as it yielded two major (a and b) and several minor phosphopeptides (Figure 4.2.2). PMA treatment strongly increased the phosphorylation of one peptide (c) while causing four new phosphopeptides to appear (indicated by circles). These data confirmed that TSC1 undergoes regulated phosphorylation in a similar fashion to TSC2 and led to speculation that it could be involved in the regulation of mTORC1 signalling.

Since $p90^{RSKs}$ did not seem to regulate mTORC1 signalling in ARVC upon activation of the MEK/Erk pathway (described in previous section), Erk was an obvious candidate for phosphorylating TSC1 in response to PMA. Based on sequence analysis, Ser1102 (RXKXXS) is the only amino acid on TSC1 that has the potential to be phosphorylated by $p90^{RSKs}$ since it partially resembles the RXRXX(S/T) consensus

$p90^{RSKs}$ substrate sequence. In contrast, TSC1 contains multiple potential Erk phosphorylation sites, which consist of a serine or threonine followed by a proline (T/SP).

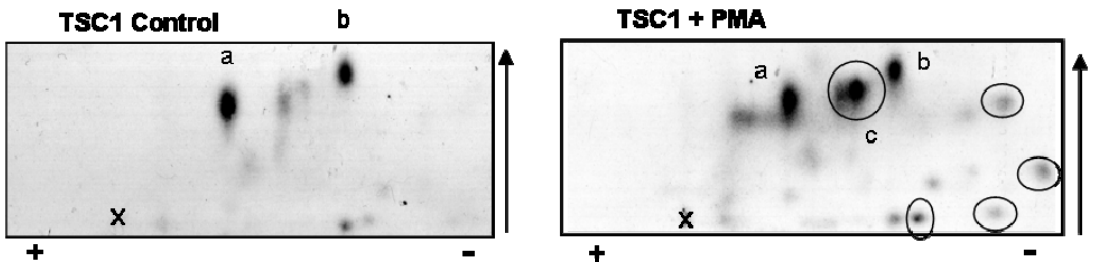

FIGURE 4.2.2. TSC1 is phosphorylated at multiple sites *in vivo*. HEK293 cells were co-transfected with vectors for FLAG-TSC1 and -TSC2. Twenty-four h later, the cells were starved of serum for 16 h and then metabolically labelled with ^{32}P-orthophosphate for 4 h. In some instances, cells were subsequently stimulated with 1 μM PMA for 25 min. Cells were harvested and radiolabelled FLAG-TSC1 and -TSC2 immunoprecipitated as described in material and methods. Immunoprecipitated proteins were resolved by SDS-PAGE. Radiolabelled FLAG-TSC1 and –TSC2 were excised from the gel and subjected to proteolytic digestion with trypsin. Tryptic peptides were separated by two-dimensional peptide-mapping and visualized by autoradiography. Positive and negative electrodes are noted by the (+) and (-) signs. *Arrow* denotes the direction of the chromatography. *Cross* marks the origin where samples were applied. Phosphorylated peptides discussed in the main text are circled.

In order to identify the kinase(s) responsible for phosphorylating TSC1 via the MEK/Erk pathway in the event of PMA stimulation, we wished to perform an *in vitro* phosphorylation assay with TSC1 and its potential kinase, Erk1. Before performing the radiolabelling assay, care was taken to make certain that the amount of purified human Mnk1, a known *in vivo* substrate of Erk1 and thus the positive control in this assay, was similar to that of the immunoprecipitated TSC1 and TSC2 so any false positive or negative conclusions are avoided. It was determined that 50 ng of Mnk1 would be suitable for subsequent experiments (Figure 4.2.3.A). In the *in vitro* [^{32}P] radiolabelling assay, activated human Erk1 was incubated with ectopically-expressed human TSC1 and TSC2 in the presence of [γ-^{32}P]ATP for different lengths of time as indicated. In the control set where no Erk1 was added, Mnk1 had no phosphorylation whereas TSC1 nearly remained unphosphorylated even when the reaction was run for 40 min indicating that the preparations of TSC1 and Mnk1 were clean and that no other active kinase was present or active. In the experimental set where activated Erk1 was added to the reaction, phosphorylation of TSC1 became apparent in 10 min and increased in intensity with time. Although the phosphorylation of TSC1 by Erk1 seems rather weak, it is certainly on a par with that of Mnk1, a genuine substrate of Erk1 *in vivo*.

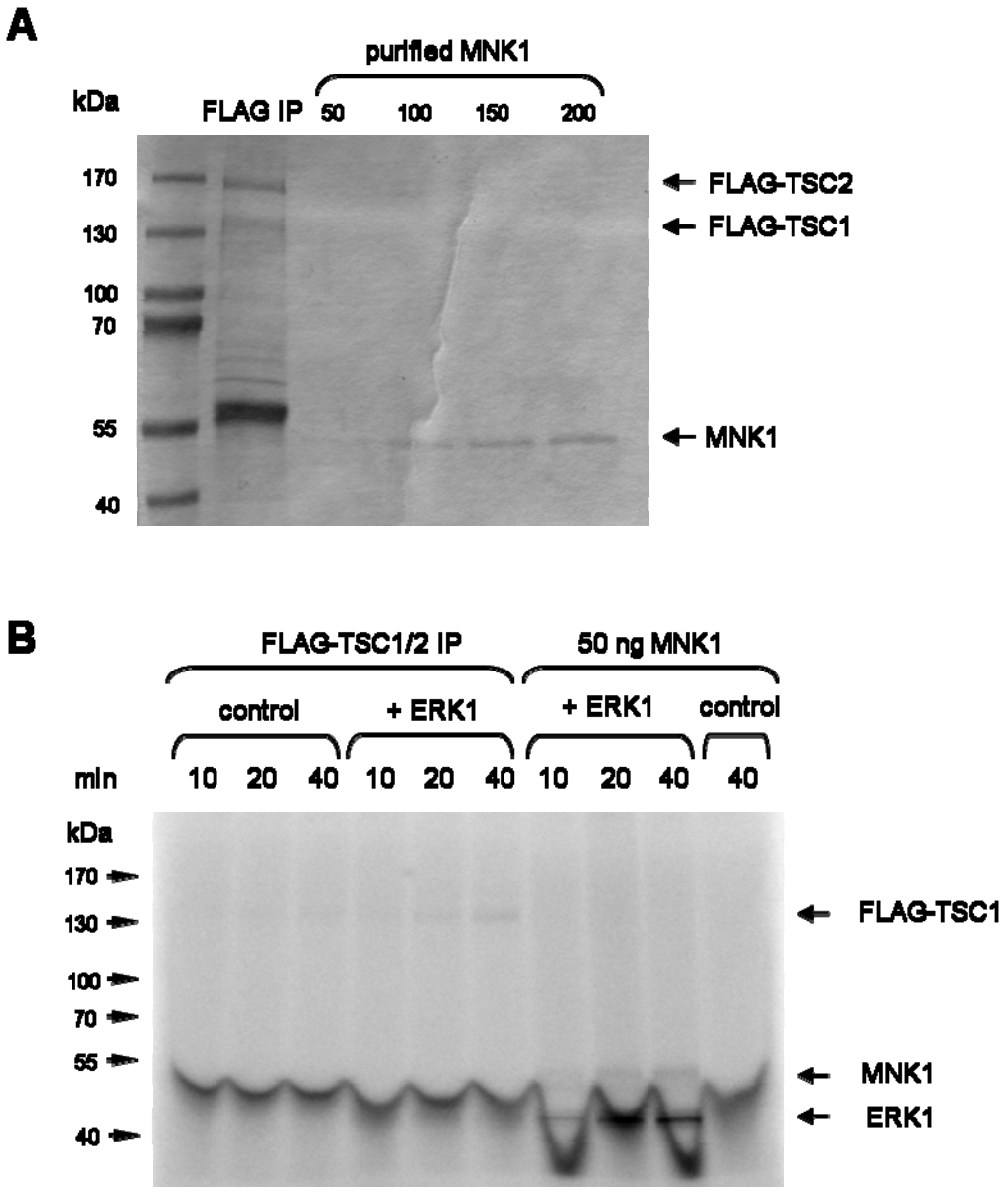

FIGURE 4.2.3. TSC1 is phosphorylated by activated Erk1 *in vitro*. (A-B) HEK293 cells were co-transfected with vectors for FLAG-TSC1 and -TSC2. Twenty-four h later, the cells were starved of serum for 16 h. Cells were harvested and FLAG-TSC1 and -TSC2 immunoprecipitated as described in material and methods. (A) Immunoprecipitated proteins were resolved by SDS-PAGE and stained with colloidal blue. (B) Immunoprecipitated FLAG-TSC1 and –TSC2 were labeled with ^{32}P-orthophosphate in the presence or absence of activated Erk1 for 60 min. Purified human Mnk1 was used as a positive control substrate for Erk1. Labelled proteins were resolved by SDS-PAGE and displayed by phosphor-imager.

To further advance our understanding of TSC1 phosphorylation by Erk1, a two-dimensional peptide map analysis was performed. TSC1 and TSC2 were immunoprecipitated with anti-flag antibody and were radiolabelled *in vitro* with [γ-^{32}P]ATP in the presence of Erk1. The radiolabelled TSC1 and TSC2 were resolved on SDS-PAGE, and the bands corresponding to TSC1 were excised and subjected to in-gel tryptic digestion. The resultant phosphopeptides were further separated by electrophoresis (1st dimension) and chromatography (2nd dimension) in a two-dimensional peptide mapping. In the control map (Figure 4.2.4), there were two phosphopeptides observed (peptides d and e). Peptide "d" was more prominently phosphorylated while peptide "e" exhibited a weaker signal. In the Erk1 map (Figure 4.2.4), the peptide map showed a total of four phosphopeptides, including the two basally phosphorylated peptides in the control map. The new peptide "c" was markedly phosphorylated by Erk1 while peptide d showed up weakly indicating that Erk1 could only phosphorylate a couple of sites on TSC1. Peptide "d" and "e" did not change in intensity implying that they are not substrates for Erk1 but rather reflect non-specific phosphorylation by contaminating kinases. In the map where TSC1 was labelled *in vivo* after PMA treatment, there were several more phosphopeptides but only one of them (peptide c) seemed to overlap with the phosphopeptides "f" in the *in vitro* map with Erk1. Given their similar mobilities in both dimensions, peptide "c" from the *in vivo* map may be the same peptide as peptide "f" from the *in vitro* map. Peptide "c" and "f" are also the most prominently phosphorylated peptides from both of the maps (Figure 4.2.4). These findings strongly suggest that Erk1

may participate in the phosphorylation of TSC1 *in vivo*. In addition, although it may not be the only kinase that phosphorylates TSC1 *in vivo*, it is likely the main regulator of TSC1 phosphorylation.

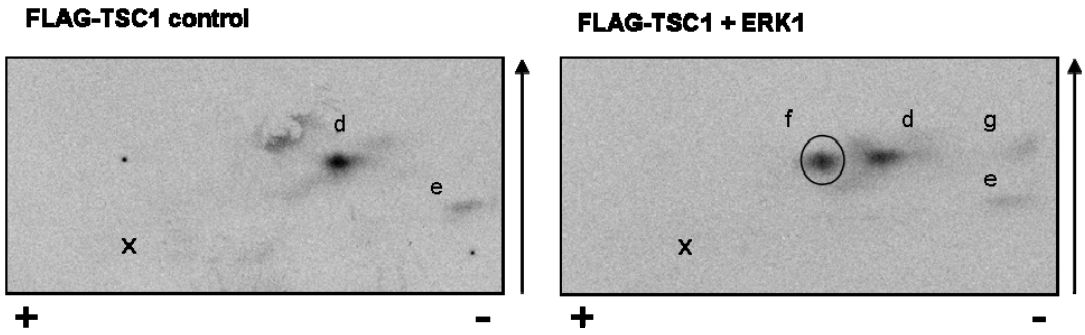

FIGURE 4.2.4. Two-dimensional peptide map analysis of TSC1 phosphorylated by Erk1 *in vitro.* HEK293 cells were co-transfected with vectors for FLAG-TSC1 and -TSC2. Twenty-four h later, the cells were starved of serum for 16 h. Cells were harvested and FLAG-TSC1 and -TSC2 immunoprecipitated as described in material and methods. Immunoprecipitated FLAG-TSC1 and –TSC2 were radiolabelled with ^{32}P-orthophosphate in the presence or absences of activated Erk1 for 60 min. Radiolabelled proteins were resolved by SDS-PAGE. Radiolabelled FLAG-TSC1 were excised from the gel and subjected to proteolytic digestion with trypsin. Tryptic peptides were separated by two-dimensional peptide-mapping and visualized by autoradiography. Positive and negative electrodes are noted by the (+) and (-) signs. *Arrow* denotes the direction of the chromatography. *Cross* marks the origin where samples were applied. The major phosphor-peptides discussed in the main text are circled.

4.3 Discussion

This section of the study centers on the upstream regulator of mTORC1 signalling, TSC1/2 complexes, and how they are in turn regulated by upstream kinases, Erk and $p90^{RSKs}$, in the MEK/Erk pathway. To investigate the functional significance of $p90^{RSKs}$, a specific $p90^{RSKs}$ inhibitor, BI-D1870, was employed (Sapkota and Cummings et al., 2007). It was discovered that $p90^{RSKs}$ is not essential for the activation of mTORC1 signalling by PE, which acts through MEK/Erk pathway (Wang and Proud, 2002), in ARVC. This implies that the $p90^{RSKs}$-induced phosphorylation of TSC2, including phosphorylation of Ser1798, also does not play a part in the upregulation of mTORC1 signalling by PE. Similar conclusions were obtained in HEK293 cells (Fonseca, 2008 unpublished). Although earlier data suggests phosphorylation of TSC2 by the MEK/Erk pathway relieves its inhibition on mTORC1 signalling (Roux and Ballif et al., 2004; Ballif and Roux et al., 2005; Rolfe and McLeod et al., 2005), our data suggest otherwise (section 4.2.1).

Although TSC2 was shown to undergo extensive phosphorylation under both basal conditions and upon the stimulation of PMA and insulin in HEK293 cells, the stimulus-induced phosphorylation appeared to be substoichiometric when the phosphopeptides were displayed on a two-dimensional map (Rolfe, 2008 unpublished). Some of the peptides were heavily phosphorylated prior to PMA or insulin stimulation and the induced phosphorylation was significantly lower than the basal phosphorylation. In fact, the phosphorylation of the peptide containing Ser1798, which is the $p90^{RSKs}$

phosphorylation site on TSC2, remains much lower than that of the basally-phosphorylated peptides in the PMA-treated cells. Since it is hard to envisage how substoichiometric phosphorylation of TSC2 could impair TSC2's constitutive GAP function sufficiently to relieve its inhibitory action on Rheb, this casts further doubt on the role of Ser1798 in the control of TSC2 and mTORC1 signalling. The quantitative proteomic data of Ballif et al. (Ballif and Roux et al., 2005) also show that the rise in Ser1798 phosphorylation is slow, continuing to rise up to one hour after addition of PMA, although activation of mTORC1 signalling appears to be more rapid than that (Herbert and Kilhams et al., 2000). Most importantly, it was shown that mutating Ser1798 to alanine on TSC2 could not inhibit the activation of mTORC1 signalling by PMA (Roux and Ballif et al., 2004).

Collectively, the above evidence argues against the idea that TSC2 is the main mediator for the activation of mTORC1 signalling by the MEK/Erk pathway. In particular, it shows that the $p90^{RSKs}$-mediated TSC2 phosphorylation does not regulate downstream mTOR signalling. Additional connections between the MEK/Erk pathway to the mTORC1 signalling may exist.

Compared to TSC2, TSC1 has received much less attention. It is entirely possible that TSC1 could be just as important as TSC2 in the context of TSC1/2 complex and mTOR signalling pathway. Until recently, TSC1 was reported to undergo complex and regulated phosphorylation receiving inputs from various upstream signalling pathways (Lee and Kuo et al., 2007). This finding supports the idea that TSC1 does not just play a

supporting role in the TSC1/2 complex and may instead actively participate in the control of its downstream signalling network, such as mTORC1 signalling. TSC1 has also been reported to be a substrate for Erk *in vivo* and *in vitro* (Ma and Chen et al., 2005). Consistent with these results, our data shows that TSC1 undergoes phosphorylation under PMA stimulation *in vivo* in HEK293 cells and Erk1 phosphorylates TSC1 *in vitro*. In fact, upon amino acid sequence analysis, there are multiple potential Erk1 phosphorylation sites (PXS/TP) in TSC1. The identification of TSC1 phosphorylation by Erk1 reveals a new avenue for the MEK/Erk pathway or other upstream pathways to regulate TSC1/2, and thus the downstream mTOR signalling network. It is now of immediate importance to identify the Erk1 phosphorylation site on TSC1 and their functional significance in the regulation of mTORC1 signalling.

Concluding Remarks and Future Directions

Deregulation of the signalling control of protein synthesis can lead to lethal conditions, such as the focus of this study, cardiac hypertrophy. Hence, it is of fundamental importance to understand the underlying molecular events that are involved in its development. According to the findings in the previous chapters, it was discovered that phenylephrine induces protein synthesis and cardiomyocyte hypertrophy independently of the action of eIF4F/4E-BP1. Although my results suggest that 4E-BP1 plays a limited role in the regulation of protein synthesis in cardiomyocytes, it does not necessarily mean that 4E-BP1 is functionally insignificant in other cell types. There is strong evidence implicating 4E-BP1 in the regulation of cell growth in both fruitflies and in some organs in mice. Futhermore, it is necessary to confirm my results by investigating 4E-BP1's role in other models of cardiac hypertrophy, such as in a whole animal model, e.g., aortic banding.

PE's effects are still highly sensitive to rapamycin treatment in the case of 4E-BP1 overexpression. This indicates that these effects depend on mTORC1 signalling. Therefore, it is likely that one or more of mTORC1 signalling substrates, such as eEF2 kinase, are involved in the activation of protein synthesis. eEF2 kinase is the only known kinase to phosphorylate and inactivate eEF2 in mammalian system. Unphosphorylated eEF2 is active and facilitates the translocation of ribosome on mRNA in the elongation step. Upon phosphorylation by eEF2 kinase, eEF2 is inactivated and elongation stalls. To understand how much of a role elongation plays in the activation of protein synthesis by

PE, it would be interesting to knock-down eEF2 kinase by small-interfering RNA and study its effect on protein synthesis and long term cell growth.

In the second half of the thesis where upstream control of mTOR signalling was explored, it was discovered that the classical MEK/Erk pathway does not require $p90^{RSKs}$ activity or the phosphorylation on Ser1798 on TSC2, but it appears to activate Erk to directly phosphorylates TSC1. It is currently unknown what molecular events lead to the inactivation of TSC1/2 complex and ultimately cause the activation of mTOR signalling. Therefore, it is important to identify the Erk phosphorylation site(s) on TSC1 by mass spectrometry. After the sites are identified, site-directed mutagenesis should be performed on those sites to generate non-phosphorylatable mutants of TSC1. Using these mutants, it will be possible to study the functional significance of Erk-directed TSC1 phosphorylation on TSC1/2 complex stability and the subsequent activation of mTOR signalling.

References:

Averous, J. and C. G. Proud (2006). "When translation meets transformation: the mTOR story." Oncogene **25** (48): 6423-35.

Ballif, B. A. and P. P. Roux, et al. (2005). "Quantitative phosphorylation profiling of the ERK/p90 ribosomal S6 kinase-signaling cassette and its targets, the tuberous sclerosis tumor suppressors." Proc Natl Acad Sci U S A **102** (3): 667-72.

Barron, A. J. and S. G. Finn, et al. (2003). "Chronic activation of extracellular-signal-regulated protein kinases by phenylephrine is required to elicit a hypertrophic response in cardiac myocytes." Biochem J **371** (Pt 1): 71-9.

Beugnet, A. and X. Wang, et al. (2003). "Target of rapamycin (TOR)-signaling and RAIP motifs play distinct roles in the mammalian TOR-dependent phosphorylation of initiation factor 4E-binding protein 1." J Biol Chem **278** (42): 40717-22.

Bogoyevitch, M. A. and J. Gillespie-Brown, et al. (1996). "Stimulation of the stress-activated mitogen-activated protein kinase subfamilies in perfused heart. p38/RK mitogen-activated protein kinases and c-Jun N-terminal kinases are activated by ischemia/reperfusion." Circ Res **79** (2): 162-73.

Bogoyevitch, M. A. and P. E. Glennon, et al. (1994). "Endothelin-1 and fibroblast growth factors stimulate the mitogen-activated protein kinase signaling cascade in cardiac myocytes. The potential role of the cascade in the integration of two signaling pathways leading to myocyte hypertrophy." J Biol Chem **269** (2): 1110-9.

Bradford, M. M. (1976). "A rapid and sensitive method for the quantitation of microgram quantities of protein utilizing the principle of protein-dye binding." Anal Biochem **72** : 248-54.

Brown, E. J. and P. A. Beal, et al. (1995). "Control of p70 s6 kinase by kinase activity of FRAP in vivo." Nature **377** (6548): 441-6.

Browne, G. J. and C. G. Proud (2002). "Regulation of peptide-chain elongation in mammalian cells." Eur J Biochem **269** (22): 5360-8.

Brunn, G. J. and C. C. Hudson, et al. (1997). "Phosphorylation of the translational repressor PHAS-I by the mammalian target of rapamycin." Science **277** (5322): 99-101.

Bueno, O. F. and W. L. De, et al. (2000). "The MEK1-ERK1/2 signaling pathway promotes compensated cardiac hypertrophy in transgenic mice." EMBO J **19** (23): 6341-50.

Burnett, P. E. and R. K. Barrow, et al. (1998). "RAFT1 phosphorylation of the translational regulators p70 S6 kinase and 4E-BP1." Proc Natl Acad Sci U S A **95** (4): 1432-7.

Cheadle, J. P. and M. P. Reeve, et al. (2000). "Molecular genetic advances in tuberous sclerosis." Hum Genet **107** (2): 97-114.

Choi, K. M. and L. P. McMahon, et al. (2003). "Two motifs in the translational repressor PHAS-I required for efficient phosphorylation by mammalian target of rapamycin and for recognition by raptor." J Biol Chem **278** (22): 19667-73.

Clerk, A. and M. A. Bogoyevitch, et al. (1994). "Differential activation of protein kinase C isoforms by endothelin-1 and phenylephrine and subsequent stimulation of p42 and p44 mitogen-activated protein kinases in ventricular myocytes cultured from neonatal rat hearts." J Biol Chem **269** (52): 32848-57.

Clerk, A. and P. H. Sugden (1999). "Activation of protein kinase cascades in the heart by hypertrophic G protein-coupled receptor agonists." Am J Cardiol **83** (12A): 64H-69H.

Cohen, P. (1996). "Dissection of protein kinase cascades that mediate cellular response to cytokines and cellular stress." Adv Pharmacol **36** : 15-27.

Drutskaya, M. S. and M. Ortiz, et al. (2005). "Inhibitory effects of tumor necrosis factor on hematopoiesis seen in vitro are translated to increased numbers of both committed and multipotent progenitors in TNF-deficient mice." Exp Hematol **33** (11): 1348-56.

Feig, L. A. and G. M. Cooper (1988). "Inhibition of NIH 3T3 cell proliferation by a mutant ras protein with preferential affinity for GDP." Mol Cell Biol **8** (8): 3235-43.

Findlay, G. M. and L. Yan, et al. (2007). "A MAP4 kinase related to Ste20 is a nutrient-sensitive regulator of mTOR signalling." Biochem J **403** (1): 13-20.

Fingar, D. C. and J. Blenis (2004). "Target of rapamycin (TOR): an integrator of nutrient and growth factor signals and coordinator of cell growth and cell cycle progression." Oncogene **23** (18): 3151-71.

Fonseca, B. D. and E. M. Smith, et al. (2007). "PRAS40 is a target for mammalian target of rapamycin complex 1 and is required for signaling downstream of this complex." J Biol Chem **282** (34): 24514-24.

Gao, X. and D. Pan (2001). "TSC1 and TSC2 tumor suppressors antagonize insulin signaling in cell growth." Genes Dev **15** (11): 1383-92.

Gillespie-Brown, J. and S. J. Fuller, et al. (1995). "The mitogen-activated protein kinase kinase MEK1 stimulates a pattern of gene expression typical of the hypertrophic phenotype in rat ventricular cardiomyocytes." J Biol Chem **270** (47): 28092-6.

Gingras, A. C. and S. P. Gygi, et al. (1999). "Regulation of 4E-BP1 phosphorylation: a novel two-step mechanism." Genes Dev **13** (11): 1422-37.

Gingras, A. C. and B. Raught, et al. (2001). "Hierarchical phosphorylation of the translation inhibitor 4E-BP1." Genes Dev **15** (21): 2852-64.

Gingras, A. C. and B. Raught, et al. (1999). "eIF4 initiation factors: effectors of mRNA recruitment to ribosomes and regulators of translation." Annu Rev Biochem **68** : 913-63.

Glennon, P. E. and S. Kaddoura, et al. (1996). "Depletion of mitogen-activated protein kinase using an antisense oligodeoxynucleotide approach downregulates the phenylephrine-induced hypertrophic response in rat cardiac myocytes." Circ Res **78** (6): 954-61.

Hamilton, T. L. and M. Stoneley, et al. (2006). "TOPs and their regulation." Biochem Soc Trans **34** (Pt 1): 12-6.

Hannan, R. D. and A. Jenkins, et al. (2003). "Cardiac hypertrophy: a matter of translation." Clin Exp Pharmacol Physiol **30** (8): 517-27.

Herbert, T. P. and G. R. Kilhams, et al. (2000). "Distinct signalling pathways mediate insulin and phorbol ester-stimulated eukaryotic initiation factor 4F assembly and protein synthesis in HEK 293 cells." J Biol Chem **275** (15): 11249-56.

Hoekstra, M. F. (1997). "Responses to DNA damage and regulation of cell cycle checkpoints by the ATM protein kinase family." Curr Opin Genet Dev **7** (2): 170-5.

Inoki, K. and Y. Li, et al. (2003). "Rheb GTPase is a direct target of TSC2 GAP activity and regulates mTOR signaling." Genes Dev **17** (15): 1829-34.

Ito, N. and G. M. Rubin (1999). "gigas, a Drosophila homolog of tuberous sclerosis gene product-2, regulates the cell cycle." Cell **96** (4): 529-39.

Jacinto, E. and R. Loewith, et al. (2004). "Mammalian TOR complex 2 controls the actin cytoskeleton and is rapamycin insensitive." Nat Cell Biol **6** (11): 1122-8.

Keith, C. T. and S. L. Schreiber (1995). "PIK-related kinases: DNA repair, recombination, and cell cycle checkpoints." Science **270** (5233): 50-1.

Kimball, S. R. (2001). "Regulation of translation initiation by amino acids in eukaryotic cells." Prog Mol Subcell Biol **26** : 155-84.

Kolch, W. (2000). "Meaningful relationships: the regulation of the Ras/Raf/MEK/ERK pathway by protein interactions." Biochem J **351 Pt 2** : 289-305.

Kozak, M. (1999). "Initiation of translation in prokaryotes and eukaryotes." Gene **234** (2): 187-208.

Laemmli, U. K. (1970). "Cleavage of structural proteins during the assembly of the head of bacteriophage T4." Nature **227** (5259): 680-5.

Lazou, A. and P. H. Sugden, et al. (1998). "Activation of mitogen-activated protein kinases (p38-MAPKs, SAPKs/JNKs and ERKs) by the G-protein-coupled receptor agonist phenylephrine in the perfused rat heart." Biochem J **332 (Pt 2)** : 459-65.

Le, B. O. and E. Petroulakis, et al. (2007). "Elevated sensitivity to diet-induced obesity and insulin resistance in mice lacking 4E-BP1 and 4E-BP2." J Clin Invest **117** (2): 387-96.

Lee, D. F. and H. P. Kuo, et al. (2007). "IKK beta suppression of TSC1 links inflammation and tumor angiogenesis via the mTOR pathway." Cell **130** (3): 440-55.

Lee, V. H. and T. Healy, et al. (2008). "Analysis of the regulatory motifs in eukaryotic initiation factor 4E-binding protein 1." FEBS J.

Li, Y. and K. Inoki, et al. (2004). "Biochemical and functional characterizations of small GTPase Rheb and TSC2 GAP activity." Mol Cell Biol **24** (18): 7965-75.

Lobert, S. and J. J. Correia (1994). "Method for rapid electrophoretic transfer of isoelectric focusing gels to polyvinylidene difluoride." Electrophoresis **15** (7): 930-1.

Long, X. and S. Ortiz-Vega, et al. (2005). "Rheb binding to mammalian target of rapamycin (mTOR) is regulated by amino acid sufficiency." J Biol Chem **280** (25): 23433-6.

Ma, L. and Z. Chen, et al. (2005). "Phosphorylation and functional inactivation of TSC2 by Erk implications for tuberous sclerosis and cancer pathogenesis." Cell **121** (2): 179-93.

Mader, S. and H. Lee, et al. (1995). "The translation initiation factor eIF-4E binds to a common motif shared by the translation factor eIF-4 gamma and the translational repressors 4E-binding proteins." Mol Cell Biol **15** (9): 4990-7.

Manning, B. D. and A. R. Tee, et al. (2002). "Identification of the tuberous sclerosis complex-2 tumor suppressor gene product tuberin as a target of the phosphoinositide 3-kinase/akt pathway." Mol Cell **10** (1): 151-62.

McMullen, J. R. and M. C. Sherwood, et al. (2004). "Inhibition of mTOR signaling with rapamycin regresses established cardiac hypertrophy induced by pressure overload." Circulation **109** (24): 3050-5.

McMullen, J. R. and T. Shioi, et al. (2004). "Deletion of ribosomal S6 kinases does not attenuate pathological, physiological, or insulin-like growth factor 1 receptor-phosphoinositide 3-kinase-induced cardiac hypertrophy." Mol Cell Biol **24** (14): 6231-40.

Miron, M. and J. Verdu, et al. (2001). "The translational inhibitor 4E-BP is an effector of PI(3)K/Akt signalling and cell growth in Drosophila." Nat Cell Biol **3** (6): 596-601.

Molkentin, J. D. and I. I. Dorn (2001). "Cytoplasmic signaling pathways that regulate cardiac hypertrophy." Annu Rev Physiol **63** : 391-426.

Montagne, J. and M. J. Stewart, et al. (1999). "Drosophila S6 kinase: a regulator of cell size." Science **285** (5436): 2126-9.

Mothe-Satney, I. and D. Yang, et al. (2000). "Multiple mechanisms control phosphorylation of PHAS-I in five (S/T)P sites that govern translational repression." Mol Cell Biol **20** (10): 3558-67.

Nojima, H. and C. Tokunaga, et al. (2003). "The mammalian target of rapamycin (mTOR) partner, raptor, binds the mTOR substrates p70 S6 kinase and 4E-BP1 through their TOR signaling (TOS) motif." J Biol Chem **278** (18): 15461-4.

Novoa, I. and L. Carrasco (1999). "Cleavage of eukaryotic translation initiation factor 4G by exogenously added hybrid proteins containing poliovirus 2Apro in HeLa cells: effects on gene expression." Mol Cell Biol **19** (4): 2445-54.

Oldham, S. and J. Montagne, et al. (2000). "Genetic and biochemical characterization of dTOR, the Drosophila homolog of the target of rapamycin." Genes Dev **14** (21): 2689-94.

Pende, M. and S. H. Um, et al. (2004). "S6K1(-/-)/S6K2(-/-) mice exhibit perinatal lethality and rapamycin-sensitive 5'-terminal oligopyrimidine mRNA translation and reveal a mitogen-activated protein kinase-dependent S6 kinase pathway." Mol Cell Biol **24** (8): 3112-24.

Pestova, T. V. and V. G. Kolupaeva, et al. (2001). "Molecular mechanisms of translation initiation in eukaryotes." Proc Natl Acad Sci U S A **98** (13): 7029-36.

Potter, C. J. and H. Huang, et al. (2001). "Drosophila Tsc1 functions with Tsc2 to antagonize insulin signaling in regulating cell growth, cell proliferation, and organ size." Cell **105** (3): 357-68.

Proud, C. G. (2004). "Ras, PI3-kinase and mTOR signaling in cardiac hypertrophy." Cardiovasc Res **63** (3): 403-13.

Purcell, N. H. and G. Tang, et al. (2001). "Activation of NF-kappa B is required for hypertrophic growth of primary rat neonatal ventricular cardiomyocytes." Proc Natl Acad Sci U S A **98** (12): 6668-73.

Radimerski, T. and J. Montagne, et al. (2002). "Lethality of Drosophila lacking TSC tumor suppressor function rescued by reducing dS6K signaling." Genes Dev **16** (20): 2627-32.

Richter-Cook, N. J. and T. E. Dever, et al. (1998). "Purification and characterization of a new eukaryotic protein translation factor. Eukaryotic initiation factor 4H." J Biol Chem **273** (13): 7579-87.

Rogers, G. W. and N. J. Richter, et al. (1999). "Biochemical and kinetic characterization of the RNA helicase activity of eukaryotic initiation factor 4A." J Biol Chem **274** (18): 12236-44.

Rolfe, M. and L. E. McLeod, et al. (2005). "Activation of protein synthesis in cardiomyocytes by the hypertrophic agent phenylephrine requires the activation of ERK and involves phosphorylation of tuberous sclerosis complex 2 (TSC2)." Biochem J **388** (Pt 3): 973-84.

Roux, P. P. and B. A. Ballif, et al. (2004). "Tumor-promoting phorbol esters and activated Ras inactivate the tuberous sclerosis tumor suppressor complex via p90 ribosomal S6 kinase." Proc Natl Acad Sci U S A **101** (37): 13489-94.

Rozen, F. and I. Edery, et al. (1990). "Bidirectional RNA helicase activity of eucaryotic translation initiation factors 4A and 4F." Mol Cell Biol **10** (3): 1134-44.

Ruvinsky, I. and O. Meyuhas (2006). "Ribosomal protein S6 phosphorylation: from protein synthesis to cell size." Trends Biochem Sci **31** (6): 342-8.

Saghir, A. N. and W. J. Tuxworth, et al. (2001). "Modifications of eukaryotic initiation factor 4F (eIF4F) in adult cardiocytes by adenoviral gene transfer: differential effects on eIF4F activity and total protein synthesis rates." Biochem J **356** (Pt 2): 557-66.

Sapkota, G. P. and L. Cummings, et al. (2007). "BI-D1870 is a specific inhibitor of the p90 RSK (ribosomal S6 kinase) isoforms in vitro and in vivo." Biochem J **401** (1): 29-38.

Sarbassov, D. D. and S. M. Ali, et al. (2004). "Rictor, a novel binding partner of mTOR, defines a rapamycin-insensitive and raptor-independent pathway that regulates the cytoskeleton." Curr Biol **14** (14): 1296-302.

Sarbassov, D. D. and S. M. Ali, et al. (2006). "Prolonged rapamycin treatment inhibits mTORC2 assembly and

Akt/PKB." Mol Cell **22** (2): 159-68.

Saucedo, L. J. and X. Gao, et al. (2003). "Rheb promotes cell growth as a component of the insulin/TOR signalling network." Nat Cell Biol **5** (6): 566-71.

Schalm, S. S. and J. Blenis (2002). "Identification of a conserved motif required for mTOR signaling." Curr Biol **12** (8): 632-9.

Schalm, S. S. and D. C. Fingar, et al. (2003). "TOS motif-mediated raptor binding regulates 4E-BP1 multisite phosphorylation and function." Curr Biol **13** (10): 797-806.

Scheffzek, K. and M. R. Ahmadian, et al. (1997). "The Ras-RasGAP complex: structural basis for GTPase activation and its loss in oncogenic Ras mutants." Science **277** (5324): 333-8.

Schmelzle, T. and M. N. Hall (2000). "TOR, a central controller of cell growth." Cell **103** (2): 253-62.

Shatkin, A. J. and A. K. Banerjee, et al. (1976). "Dependence of translation on 5'-terminal methylation of mRNA." Fed Proc **35** (11): 2214-7.

Shima, H. and M. Pende, et al. (1998). "Disruption of the p70(s6k)/p85(s6k) gene reveals a small mouse phenotype and a new functional S6 kinase." EMBO J **17** (22): 6649-59.

Shioi, T. and J. R. McMullen, et al. (2003). "Rapamycin attenuates load-induced cardiac hypertrophy in mice." Circulation **107** (12): 1664-70.

Stocker, H. and T. Radimerski, et al. (2003). "Rheb is an essential regulator of S6K in controlling cell growth in Drosophila." Nat Cell Biol **5** (6): 559-65.

Tang, H. and E. Hornstein, et al. (2001). "Amino acid-induced translation of TOP mRNAs is fully dependent on phosphatidylinositol 3-kinase-mediated signaling, is partially inhibited by rapamycin, and is independent of S6K1 and rpS6 phosphorylation." Mol Cell Biol **21** (24): 8671-83.

Tee, A. R. and D. C. Fingar, et al. (2002). "Tuberous sclerosis complex-1 and -2 gene products function together to inhibit mammalian target of rapamycin (mTOR)-mediated downstream signaling." Proc Natl Acad Sci U S A **99** (21): 13571-6.

Tee, A. R. and B. D. Manning, et al. (2003). "Tuberous sclerosis complex gene products, Tuberin and Hamartin, control mTOR signaling by acting as a GTPase-activating protein complex toward Rheb." Curr Biol **13** (15): 1259-68.

Thomas, G. and M. N. Hall (1997). "TOR signalling and control of cell growth." Curr Opin Cell Biol **9** (6): 782-7.

Tsukiyama-Kohara, K. and F. Poulin, et al. (2001). "Adipose tissue reduction in mice lacking the translational inhibitor 4E-BP1." Nat Med **7** (10): 1128-32.

Tuxworth, W. J. and A. N. Saghir, et al. (2004). "Regulation of protein synthesis by eIF4E phosphorylation in adult cardiocytes: the consequence of secondary structure in the 5'-untranslated region of mRNA." Biochem J **378** (Pt 1): 73-82.

Wang, L. and I. Gout, et al. (2001). "Cross-talk between the ERK and p70 S6 kinase (S6K) signaling pathways. MEK-dependent activation of S6K2 in cardiomyocytes." J Biol Chem **276** (35): 32670-7.

Wang, L. and C. G. Proud (2002). "Ras/Erk signaling is essential for activation of protein synthesis by Gq protein-coupled receptor agonists in adult cardiomyocytes." Circ Res **91** (9): 821-9.

Wang, L. and C. G. Proud (2002). "Ras/Erk signaling is essential for activation of protein synthesis by Gq protein-coupled receptor agonists in adult cardiomyocytes." Circ Res **91** (9): 821-9.

Wang, L. and C. G. Proud (2002). "Regulation of the phosphorylation of elongation factor 2 by MEK-dependent signalling in adult rat cardiomyocytes." FEBS Lett **531** (2): 285-9.

Wang, L. and M. Rolfe, et al. (2003). "Ca(2+)-independent protein kinase C activity is required for alpha1-adrenergic-receptor-mediated regulation of ribosomal protein S6 kinases in adult cardiomyocytes." Biochem J **373** (Pt 2): 603-11.

Wang, L. and X. Wang, et al. (2000). "Activation of mRNA translation in rat cardiac myocytes by insulin involves multiple rapamycin-sensitive steps." Am J Physiol Heart Circ Physiol **278** (4): H1056-68.

Wang, X. and A. Beugnet, et al. (2005). "Distinct signaling events downstream of mTOR cooperate to mediate the effects of amino acids and insulin on initiation factor 4E-binding proteins." Mol Cell Biol **25** (7): 2558-72.

Wang, X. and W. Li, et al. (2003). "The C terminus of initiation factor 4E-binding protein 1 contains multiple regulatory features that influence its function and phosphorylation." Mol Cell Biol **23** (5): 1546-57.

Wang, X. and C. G. Proud (2006). "The mTOR pathway in the control of protein synthesis." Physiology (Bethesda) **21** : 362-9.

Wang, X. and C. G. Proud (2008). "A novel mechanism for the control of translation initiation by amino acids, mediated by phosphorylation of eukaryotic initiation factor 2B." Mol Cell Biol **28** (5): 1429-42.

Wu, Y. and B. P. Zhou (2007). "Kinases meet at TSC." Cell Res **17** (12): 971-3.

Wullschleger, S. and R. Loewith, et al. (2006). "TOR signaling in growth and metabolism." Cell **124** (3): 471-84.

Yamazaki, T. and K. Tobe, et al. (1993). "Mechanical loading activates mitogen-activated protein kinase and S6 peptide kinase in cultured rat cardiac myocytes." J Biol Chem **268** (16): 12069-76.

Yue, T. L. and J. L. Gu, et al. (2000). "Extracellular signal-regulated kinase plays an essential role in hypertrophic agonists, endothelin-1 and phenylephrine-induced cardiomyocyte hypertrophy." J Biol Chem **275** (48): 37895-901.

Zhang, H. and J. P. Stallock, et al. (2000). "Regulation of cellular growth by the Drosophila target of rapamycin dTOR." Genes Dev **14** (21): 2712-24.

Zhang, Y. and X. Gao, et al. (2003). "Rheb is a direct target of the tuberous sclerosis tumour suppressor proteins." Nat Cell Biol **5** (6): 578-81.